DISCHARGE COEFFICIENTS FOR BROAD-CRESTED WEIRS OF LOW ASPECT RATIOS

by

Carl Anderson

Thesis submitted to the Graduate Faculty of the
Virginia Polytechnic Institute
in candidacy for the degree of

MASTER OF SCIENCE
in
Civil Engineering

APPROVED:

Chairman, Dr. R.M. Sorenson

Dr. J.M. Wiggert

Dr. R.A. Comparin

Dr. H. M. Morris

June, 1967

Blacksburg, Virginia

TABLE OF CONTENTS

LIST OF FIGURES

LIST OF TABLES

LIST OF SYMBOLS

B = actual crest width

B_{eff} = effective crest width

C = discharge coefficient

C_o = theoretical value of C for L=H

cfs = cubic feet per second

D = reattachment distance

d = distance from crest entrance to maximum separation height

E = specific energy

E_c = critical specific energy

g = acceleration due to gravity

H = total head

h = maximum separation height

K = coefficient

L = length of weir crest

ℓ = effect length of crest boundary layer

ℓ_o = theoretical value of for L=H

P = weir height from channel invert

Q = total discharge

q = unit discharge

R_H = Reynolds number $\frac{v_c H}{\nu}$

R = Reynolds number $\frac{v_c \ell}{\nu}$

v_c = critical velocity

y_c = critical depth

δ = boundary layer disturbance thickness

δ^* = boundary layer displacement thickness

ν = kinematic viscosity

(Subscripts are used as follows: TH = theoretical; EX = experimental; i = ideal; a = actual; max = maximum.)

I ACKNOWLEDGEMENTS

The author wishes to express his thanks to , thesis advisor, for his assistance in the selection of a thesis topic, in the laboratory, and in the writing of the thesis; to , for his practical suggestions in assembling the laboratory apparatus, and for his comments during the writing of the thesis; and to n of the Mechanical Engineering Department, for his suggestions during the experimentation and, as a professor, for his role in the author's understanding of boundary layer phenomena; and to for the typing of this thesis.

II INTRODUCTION

The importance of overfall weirs is due to their ability to act as discharge meters in open channel flow. Extensive experimental investigation of weir flow has been conducted in the past and numerous experimental data have been accumulated for weirs of all types.

The customary approach has been experimental, however, and completely theoretical treatments of the problem of discharge over weirs have not been successful. The discharge has always been expressed as the product of the ideal discharge and an experimentally determined discharge coefficient. The ideal discharge can be obtained for sharp-crested weirs by an integration of Torricelli's theorem (11), or by a specific energy approach for broad-crested weirs (Sec. IV). The discharge coefficient has customarily been determined by experiments.

The experimental determination of the discharge coefficient provides rating curves or empirical rating equations for individual weirs, but does not provide a means for predicting the coefficient for weirs of similar type with slightly different geometry. The theoretical development of accurate, general discharge equations for weirs would be an important contribution to the field of open channel flow measurement.

Broad-crested weirs are frequently used in irrigation works because they can operate as flow meters with very little loss of total head (22). A completely theoretical analysis of the discharge over such weirs would appear to involve less difficulty than that for sharp-crested weirs due to the existence of nearly parallel flow on the broad crest.

G.W. Hall attempted such an anlysis for broad-crested weirs with horizontal crests and square entrances, and extended his approach to include the effects of side walls on the discharge (7). Experimental data were found to support the analysis for weirs possessing two-dimensional flow, but none were available to show the effects of side walls. This thesis describes an attempt to verify Hall's theoretical analysis of the effects of side walls on the discharge of broad-crested weirs.

The symbols and terminology used by Hall (7) have been retained (p.5). The term "crest length" is used to refer to the dimension of the weir crest measured parallel to the flow. "Crest width" means the dimension of the weir crest measured perpendicular to the flow. Broad-crested weirs having crest widths equal to the width of the approach channel are referred to as suppressed weirs, while weirs having crest widths less than that of the approach channel are contracted weirs.

III REVIEW OF LITERATURE

The experiments by Blackwell (2,11) in 1850 are the first recorded investigation of broad-crested weirs. Blackwell's tests included three experiments with contracted broad-crested weirs having square entrances and moderately rough horizontal crests of varying widths. The discharges were measured volumetrically by means of a gaging tank. Blackwell's results were reported as experimental values of the discharge coefficient C from the equation $q = C H^{3/2}$, in which q is the unit discharge and H is the total upstream head on the weir. No theoretical analysis of the discharge coefficient was attempted.

Bazin (11,19), in 1896, performed a series of experiments on weirs of various types including three suppressed broad-crested weirs with horizontal crests and square entrances. The heads on the weirs were measured by float gages in stilling wells connected to the test channel by pipes. The discharges were measured volumetrically in a gaging basin. Bazin's results were also reported as the experimental values of the discharge coefficient C from the equation $q = C H^{3/2}$.

Horton (11) conducted a series of tests on broad-crested weirs in 1903 for the U.S. Geological Survey at the Cornell University Hydraulics Laboratory. Seven suppressed

broad-crested weirs with horizontal crests and square entrances were tested in a long outdoor open channel. A standard weir was used to measure the discharge and the heads on the test weirs were measured by open manometers connected to piezometer taps in the bottom of the channel. Horton presented his results as the experimentally determined values of the coefficient C, and also reported the data of Blackwell and Bazin.

Woodburn (22) conducted a series of broad-crested weir experiments at the University of Michigan in 1928, including thirty-seven tests of a suppressed broad-crested weir with a horizontal crest and square entrance edge. The tests were performed in an open flume using a standard weir to measure the discharge. Woodburn presented the resulting experimental values of the coefficient C and compared them with similar coefficients of Bazin and Horton.

Two theoretical approaches to the determination of the discharge coefficients for broad-crested weirs were attempted by Delleur and Hall, both of whom based their analyses on boundary layer theory.

Delleur (5) used the continuity, energy and momentum equations for the boundary layer to predict the discharge coefficient for a weir crest with a rounded entrance and no entrance separation. Delleur's approach gave coefficients which were higher than those of Hall (7), who

assumed separated entrance flow and a flat-plate boundary layer development. Delleur's analysis did not include the effects of side walls on the discharge coefficient as did Hall's approach to the problem (Sec. IV).

IV THEORETICAL CONSIDERATIONS

Two-dimensional Case

The general equation for the discharge over a broad-crested weir terminating in a free overfall (Fig. 1) is derived from energy considerations.

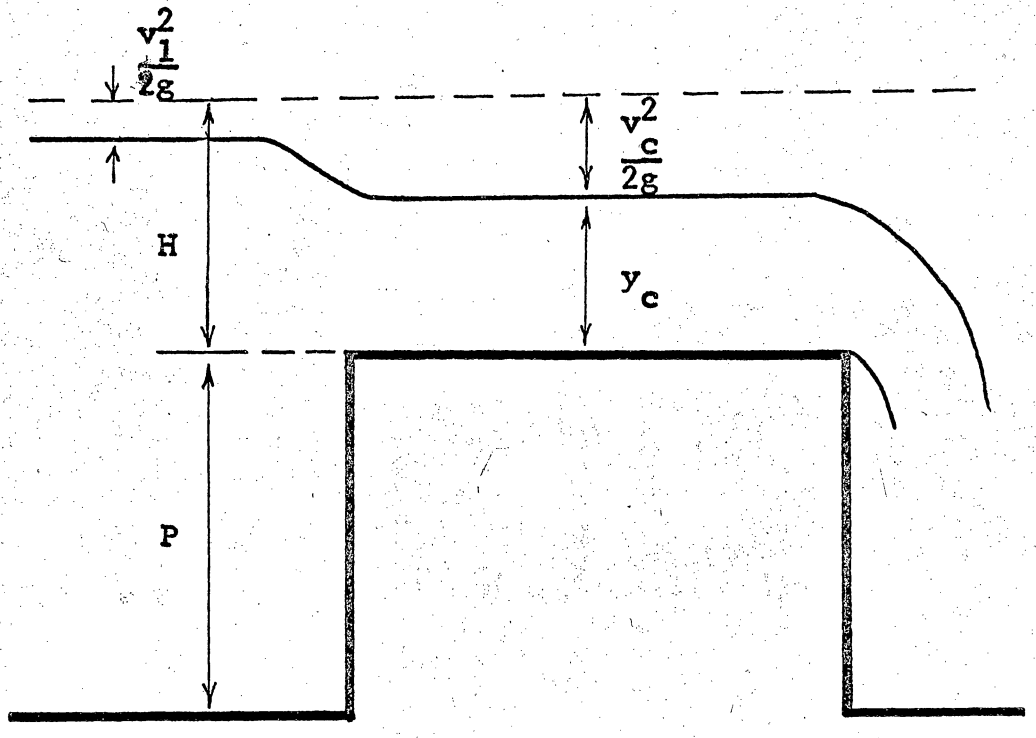

Figure 1. Ideal Flow over a Broad-crested Weir.

If the crest is horizontal, as is shown in Fig. 1, the presence of the free overfall insures that critical flow will exist somewhere on the crest (10).

If energy losses due to surface friction and separation are neglected, and if parallel flow is assumed to exist on

the weir crest, the critical specific energy E_c will be equal to H, the total upstream head on the weir. Thus,

$$E_c = H \tag{1}$$

Also, as is shown in Appendix A, for rectangular channels,

$$y_c = \frac{2}{3} H \tag{2}$$

and

$$v_c = \sqrt{\frac{2}{3} g H} \tag{3}$$

where y_c is the critical depth, v_c is the average velocity at critical flow, and g is the acceleration due to gravity.

The ideal unit discharge q_i over the broad-crested weir is then given by

$$q_i = v_c y_c = \frac{2}{3} H \sqrt{\frac{2}{3} g H} \tag{4}$$

or

$$q_i = \left(\frac{2}{3}\right)^{3/2} \sqrt{g}\, H^{3/2} \tag{5}$$

The actual unit discharge q_a can be expressed as a product of the ideal discharge and a discharge correction coefficient C, i.e.,

$$q_a = C q_i = \left(\frac{2}{3}\right)^{3/2} C \sqrt{g}\, H^{3/2} \tag{6}$$

The discharge coefficient accounts for the reduction in discharge due to friction and form losses, and the existence of a nonhydrostatic pressure distribution on the weir crest.

Hall's theoretical analysis (7) of the discharge coefficient C is for a two-dimensional, square-entranced, broad-crested weir with a horizontal crest and a total upstream head H. The theory is presented here without comment; discussion of the validity of certain of its assumptions follows in Section VI.

Hall assumes that the actual discharge per unit width q_a is equivalent to the ideal unit discharge that would occur under a head $H-\delta^*_{max}$, where δ^*_{max} is the maximum displacement thickness of the crest boundary layer. Thus,

$$q_a = (\tfrac{2}{3})^{3/2} \sqrt{g}\ (H - \delta^*_{max})^{3/2} \tag{7}$$

or

$$q_a = (\tfrac{2}{3})^{3/2} \sqrt{g}\ H^{3/2}\ (1 - \frac{\delta^*_{max}}{H})^{3/2} \tag{8}$$

By comparing Eqs. (5) and (8),

$$C = (1 - \frac{\delta^*_{max}}{H})^{3/2} \tag{9}$$

and if $\frac{\delta^*_{max}}{H}$ can be considered small when compared to unity,

$$C = 1 - \frac{3}{2} \frac{\delta^*_{max}}{H} \tag{10}$$

by a binomial expansion of the right hand term of Eq. (9).

Thus, the theoretical evaluation of the coefficient C requires an analysis of the boundary layer on the weir crest. Hall assumes the crest boundary layer development to

be equivalent to that of a turbulent boundary layer on a semi-infinite, smooth flat plate at zero incidence and with zero pressure gradient. Outside the boundary layer, it is assumed that a uniform-velocity, parallel-flow field exists with velocity equal to the theoretical critical velocity v_c, from Eq. (3).

Assuming a $\frac{1}{7}$-power law velocity distribution, the growth of the boundary layer disturbance thickness δ on a flat smooth plate is given by

$$\delta(x) = 0.37 \times R_x^{-0.2} \tag{11}$$

where $R_x = \frac{v_c x}{\nu}$ is a Reynolds number based on the free stream velocity v_c and x, the distance from the leading edge of the plate (20).

Also, for the assumed $\frac{1}{7}$-power law velocity distribution, $\delta^* = \frac{\delta}{8}$. Therefore,

$$\delta^*(x) = 0.0463 \times R_x^{-0.2} \tag{12}$$

In the case of a broad-crested weir with a square entrance, a separation region occurs at the crest entrance as shown in Fig. 2. The separation region causes the origin of the equivalent flat plate boundary layer to be located at some virtual position upstream of the weir instead of at the crest edge. (Fig. 2) The maximum displacement thickness of the equivalent flat plate boundary layer occurs approximately at $x = \ell$. Thus,

$$\delta^*_{max} = 0.0463 \left(\frac{v_c \ell}{\nu}\right)^{-0.2} \tag{13}$$

and

$$1-C = \frac{3}{2}\,\frac{\ell}{H}\,0.0463\,R_{\ell}^{-0.2} \qquad (14)$$

Multiplying and dividing by $(\frac{\ell}{H})^{0.2}$, Eq. (14) can be rewritten as

$$1-C = 0.0690\,(\frac{\ell}{H})^{0.8}\,(\frac{v_c H}{\nu})^{-0.2} = 0.0690\,(\frac{\ell}{H})^{0.8}\,R_H^{-0.2} \qquad (15)$$

with the Reynolds number now based on v_c and the total head H.

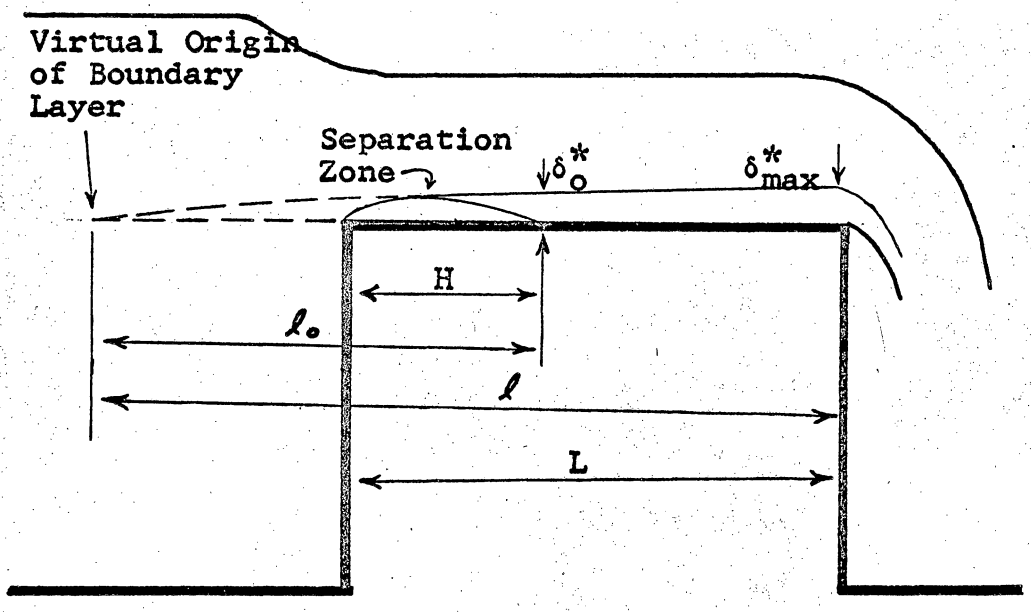

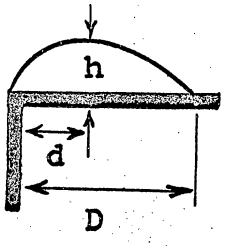

Detail of Separation Zone

Figure 2. Simplified Real Flow Model.

The virtual coordinate ℓ must now be evaluated in terms of H and the crest length L. For this purpose, Hall assumes that at a distance x=H downstream from the crest edge, the boundary layer is fully turbulent and has a displacement thickness δ_o^* equal to the maximum height, h, of the separation region. The height of the separation region h (and hence δ_o^*) is assumed to be 0.109 H, on the basis of an analogy to the underside of the nappe of a sharp-crested weir (9).

Thus for a broad-crested weir of length L=H, from Eq. (9),

$$C = (1-0.109)^{3/2} = 0.841$$

with $\delta^*_{max} = \delta_o^*$ occurring at a distance ℓ_o from the virtual origin of the flat plate boundary layer. (Fig. 2). Substituting into Eq. (15),

$$1-0.841 = 0.0690 \left(\frac{\ell_o}{H}\right)^{0.8} R_H^{-0.2}$$

$$\left(\frac{\ell_o}{H}\right)^{0.8} = 2.29\, R_H^{0.20}$$

and

$$\left(\frac{\ell_o}{H}\right) = 2.84\, R_H^{0.25} \qquad (16)$$

From the geometry of the weir as is shown in Fig. 2,

$$\ell = \ell_o + L - H \qquad (17)$$

and

$$\frac{\ell}{H} = \frac{\ell_o}{H} + \frac{L}{H} - 1 = \frac{L}{H} - 1 + 2.84\, R_H^{0.25} \qquad (18)$$

Therefore, the discharge coefficient C may be expressed in terms of L and H as

$$1-C = 0.0690 \left(\frac{L}{H} - 1 + 2.84\, R_H^{0.25}\right)^{0.80} R_H^{-0.2} \qquad (19)$$

For a weir of finite height P, this expression may be rewritten as

$$1-C = 0.0690 \left(\frac{L}{H} - 1 + K\, R_H^{0.25}\right)^{0.80} R_H^{-0.2} \qquad (20)$$

where K is a function of the ratio $\frac{H}{H+P}$. For a weir of infinite height, $\frac{H}{H+P} = 0$ and K = 2.84. Hall gives the values of K shown as a function of $\frac{H}{H+P}$ in Table 1.

Table 1. Coefficient K as a Function of $\frac{H}{H+P}$.

$\frac{H}{H+P}$	K
0	2.84
0.1	2.83
0.2	2.79
0.3	2.73
0.4	2.64
0.5	2.52
0.6	2.35
0.7	2.11
0.8	1.80
0.9	1.32

Hall states that the assumption $\frac{\delta^*}{H} = 0.109$ is valid for Reynolds numbers R_H from 50,000 to 600,000 and for $\frac{L}{H}$ ratios of approximately 3 to 33.

Three-dimensional Case

The effect of side walls, which is to decrease the discharge for a given head H, is due to the development of boundary layers on the walls. Such three-dimensional effects are accounted for by a second discharge coefficient C_B. Thus, the total discharge Q over a broad-crested weir of finite width B is given by Hall as

$$Q = C_B q_a B \tag{21}$$

where

$$q_a = C q_i = C\left(\frac{2}{3}\right)^{3/2} \sqrt{g}\, H^{3/2} \tag{5}$$

and

$$C_B = \frac{B_{eff}}{B} \tag{22}$$

B_{eff} is the effective crest width and is assumed to be equal to $B-2\delta^*_{max}$, where δ^*_{max} is the maximum displacement thickness of the wall boundary layer. Thus,

$$C_B = 1 - \frac{2\delta^*_{max}}{B} \tag{23}$$

and

$$1-C_B = \frac{2\delta^*_{max}}{B} = \frac{2H}{B}\,\frac{\delta^*_{max}}{H} \tag{24}$$

From Eq. (10),

$$\frac{\delta^*_{max}}{H} = \frac{2}{3}(1-C)$$

and if the boundary layer development on the walls is assumed to be the same as that on the crest, i.e., if the weir is a severely contracted weir,

$$1-C_B = \frac{4}{3}\frac{H}{B}(1-C) \tag{25}$$

and

$$C_B = 1-\frac{4}{3}\frac{H}{B}(1-C) \tag{26}$$

The ratio $\frac{B}{H}$ is the aspect ratio of the weir. The smallness of the aspect ratio reflects the relative importance of three-dimensional or side-wall effects.

The equation for the total discharge over the weir is then

$$Q = C_{TH}B(\frac{2}{3})^{3/2}\sqrt{g}\,H^{3/2} \tag{27}$$

in which $C_{TH} = CC_B$.

The coefficient C_B approaches unity as the aspect ratio of the weir becomes large. Selecting 0.95 as the value of C_B below which side wall effects are assumed significant, Eq. (26) determines the range of aspect ratios $\frac{B}{H}$ for which the weir must be analyzed as a three dimensional weir. Solving Eq. (26) for $\frac{B}{H}$ with $C_B = 0.95$ and $C \approx 0.70$, three-dimensional flow is defined to exist for aspect ratios $\frac{B}{H}$ less than 8.

V THE INVESTIGATION

Object of the Investigation

The object of the experimental investigation was to study the application of Hall's theoretical analysis to broad-crested weirs of low aspect ratio, and to quantitatively investigate the geometry of the crest entrance separation zone. An analysis of broad-crested weir data from the literature was also made in an attempt to verify Hall's analysis of the two-dimensional case.

Method of Investigation

Apparatus. A broad-crested weir was designed to operate in the range of Reynolds numbers and L/H ratios given by Hall as the range of reasonable accuracy of his analysis in the two-dimensional case.

The weir was constructed in a 30-foot tilting flume, which was constructed of varnished plywood. The flume was 3.0 feet wide and 2.0 feet deep. The tilting feature of the flume was used only to insure that the weir crest remained horizontal throughout the tests.

Water was supplied to the flume by a closed, gravity-head system. Two vertical turbine pumps supplied water to a constant-head tank approximately 50 feet above the flume, which in turn supplied water to the flume at discharges of

up to 1.5 cfs. The discharge into the flume was controlled by a butterfly valve and was measured by a venturi meter installed in the supply line.

The venturi meter was equipped with two 80-inch U-tube manometers, one containing mercury and the other containing a manometer fluid of specific gravity 2.95. The venturi meter was calibrated before the tests and rating equations were obtained for both manometers. (See Appendix C). For discharges up to approximately 0.6 cfs, the U-tube containing manometer fluid was used, while discharges from 0.6 cfs up to the maximum of approximately 1.5 cfs were measured using the mercury U-tube manometer.

Water was admitted to the flume through a diffusing box at the flume's upstream end. The box was fitted with three ¼-in. mesh wire screens spaced 6 in. apart to promote a uniform velocity distribution.

The upstream face of the weir was located 24.75 feet downstream from the last of the screens.

The weir itself was constructed of ½-in. acrylic sheet and had square entrance edges and equal end contractions. The weir crest length L was 3.0 feet, the crest width B, 0.75 feet, and the height P, 1.0 foot. (See Fig. 3) The upstream and downstream faces of the weir were constructed of ½-in. varnished marine plywood. The acrylic sheet was used in the construction of the weir to obtain a hydraulically

smooth surface and because its transparency would allow observation of the flow.

Head measurements were made by two open manometers connected to flush piezometer taps in the bottom of the flume. The taps were located on the flume centerline at distance of 2.5 and 10.5 feet upstream of the upstream face of the weir.

Provision was made for introducing dye into the flow at various points on the weir crest. Fifteen $\frac{1}{32}$-in. diameter dye holes were placed along the weir crest centerline at $\frac{1}{2}$-in. intervals, beginning at the upstream edge of the crest. Also, nine similar dye holes were symmetrically situated at one inch intervals along the crest entrance edge $\frac{1}{8}$-in. below the crest on the vertical upstream face, with the center hole falling on the weir centerline. (Fig. 4).

The dye, a concentrated potassium permanganate solution, was conducted to the delivery holes from an elevated dye reservoir by means of plastic tubes. The rate of delivery was regulated by a small brass plug valve in the dye feed line. The dye could be delivered to either series of holes separately or to all 24 holes at once by the use of selection valves as desired by the experimenter. (Fig.5)

A contracted, sharp-crested rectangular weir 0.75 feet wide was also tested. The weir was installed in the

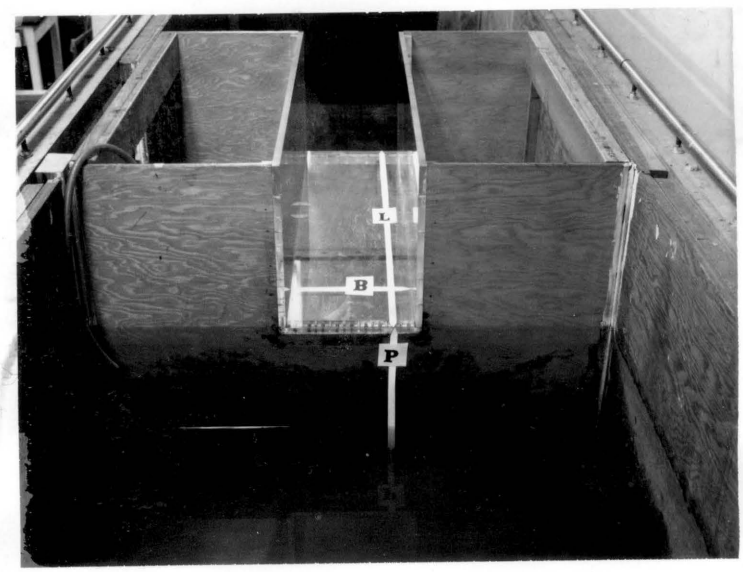

Figure 3. General View of Experimental Weir.

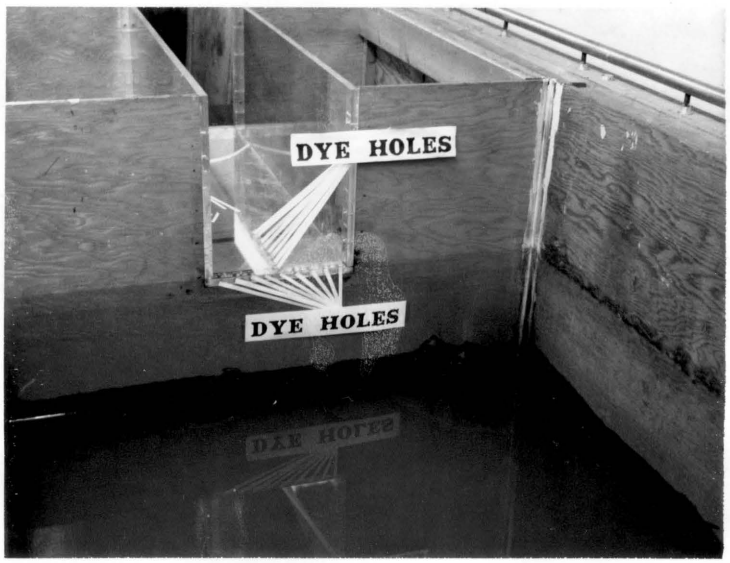

Figure 4. Experimental Weir Showing Dye Holes.

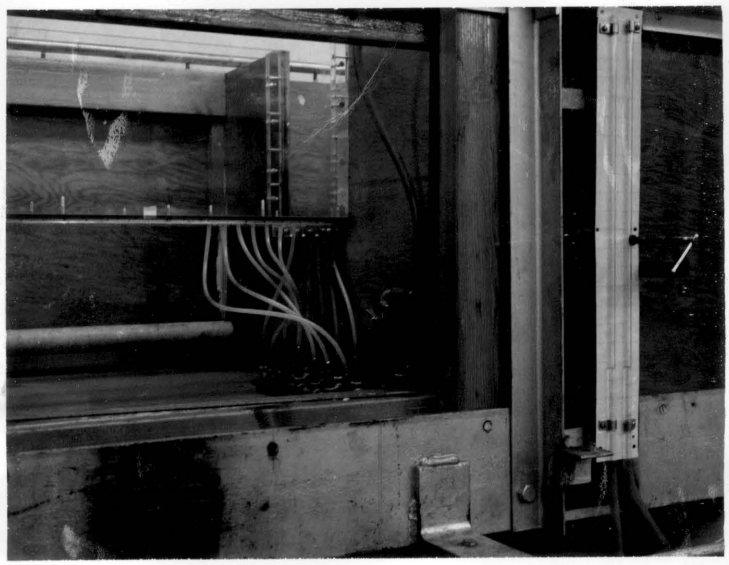

Figure 5. Experimental Weir Showing Dye Tubes.

Figure 6. Experimental Weir Discharging Water at 1.3 cfs.

rectangular opening created by removing the broad-crested weir and its downstream face from the flume. A sheet metal weir crest was installed in the opening so the weir would have equal end contractions and a height P of 1.0 foot.

Testing Procedure. Six test runs were performed, five with the broad-crested weir (Runs 1,2,3,5, and 6) and one with the sharp-crested rectangular weir (Run 4). The tests involving the broad-crested weir were repeated in order to improve upon the consistency of the results.

At the beginning of Run 1, the open manometers were zeroed with the channel empty, using the channel bottom as datum. Prior to each of the following tests, the manometer adjustment was checked with the weir crest as zero datum. In this way, the head H could be observed directly.

Preceding each test run the weir crest was checked with a carpenter's level to insure that it remained horizontal. The open manometers were also checked for alignment with the vertical using the carpenter's level.

Water was then admitted to the flume at the maximum discharge selected for the particular test run. After allowing three to five minutes for steady flow to become established, the head and venturi meter manometers were read. The discharge was then reduced sufficiently by means of the discharge regulating valve to produce the desired

head for the next observation. After another three to five minute pause, head and discharge readings were again taken. The temperature of the water was also measured to the nearest 0.5°F using a mercury thermometer.

Head and venturi meter manometer readings were estimated to the nearest 0.01 inch. Both head manometers were read to verify that the one closer to the weir was unaffected by the drawdown of the water surface at the entrance to the weir.

During Runs 5 and 6, dye was injected in order to observe the crest entrance separation region. The series of dye holes on the weir crest centerline were used to observe the reattachment point of the separated flow. For this purpose, the point was noted at which the dye was no longer swept downstream but moved upstream along the crest with the backflow of the separation zone. The distance D from the crest edge to this point was measured visually to the nearest 0.01 foot by reference to a scale on the outside of the weir.

The dye holes along the crest entrance edge were used to observe the maximum height h of the separation zone and the distance d along the crest at which the maximum occurred. These measurements were also made visually to the nearest 0.01 foot by reference to scales attached to the side wall.

During these measurements, the dye injection rate

was maintained within the range over which small variations in the rate did not alter the shape of the observed separation zone but only varied the intensity of the color imparted to the flow.

Results

The results of the experimental investigation are plotted in Figs. 7 through 27 and tabulated in Appendix D.

Fig. 7 shows the theoretical variation of the discharge coefficients C, C_B, and C_{TH}, and the ratios $\frac{L}{H}$ and $\frac{B}{H}$, as functions of the Reynolds number R_H.

Figs. 8 through 12 show the theoretical coefficient C_{TH} and the experimental coefficient C_{EX} as functions of the Reynolds number R_H for the broad-crested weir test Runs 1, 2, 3, 5, and 6. Figs. 13 and 14 show the results of the dye studies of the crest separation zone from Runs 5 and 6. The ratios $\frac{d}{H}$, $\frac{D}{H}$, and $\frac{h}{H}$ are plotted as functions of the Reynolds number in Fig. 13. The ratios $\frac{h}{d}$ and $\frac{d}{D}$ are plotted in Fig. 14 as functions of the Reynolds number.

Fig. 15 is a plot of the discharge coefficient of the sharp-crested rectangular weir as a function of Reynolds number and includes for reference, C_{EX} from test Run 5.

The results of the analysis of data from the literature on the basis of Hall's theory for two-dimensional weirs are given in Figs. 16 through 29. The theoretical and

experimental coefficients C_{TH} and C_{EX} and the ratio $\frac{L}{H}$ are plotted as functions of the Reynolds number R_H. The range of aspect ratios $\frac{B}{H}$ encountered in these data, with the exception of Woodburn's Series A, was approximately 4 to 200 compared to a range of 1 to 10 for the experimental three-dimensional weir.

The data which were analyzed were those from Blackwell's Weirs 10,11, and 12; Bazin's Series 113, 114, and 115; Horton's Cornell Hydraulic Laboratory U.S.G.S. Series 41, 42, 43, 43a, 44, 45, and 46; and Woodburn's Series A.

Experiments reported in the literature usually lacked water temperature information, so a temperature of 64.5°F was assumed. Blackwell's report did not specify the height of the weir P. A height of 3.0 feet was taken from his drawings to facilitate the analysis.

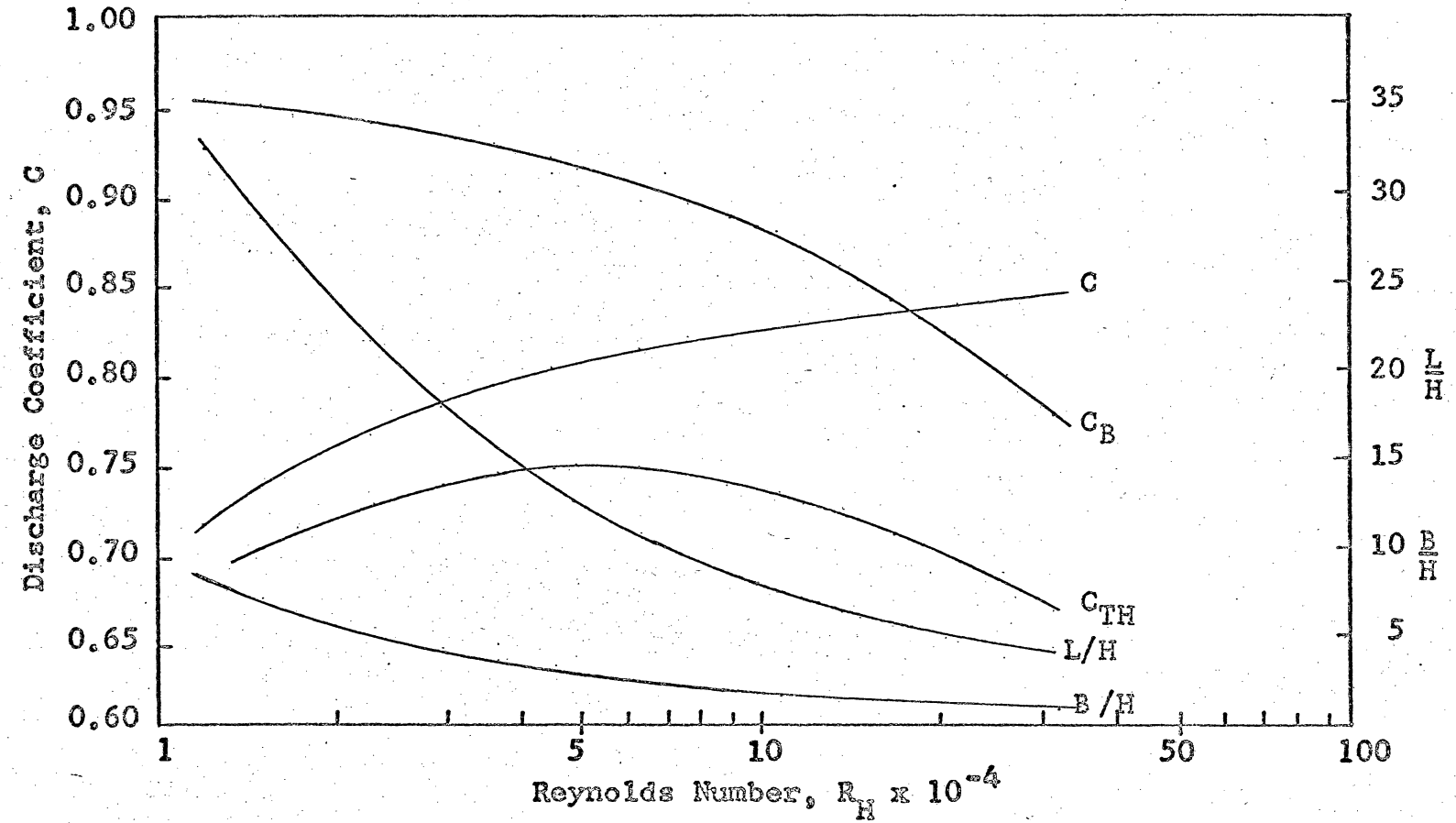

Figure 7. Theoretical Coefficients C, C_B, C_{TH} and Ratios L/H and B/H as Functions of the Reynolds number R_H for the Experimental Weir.

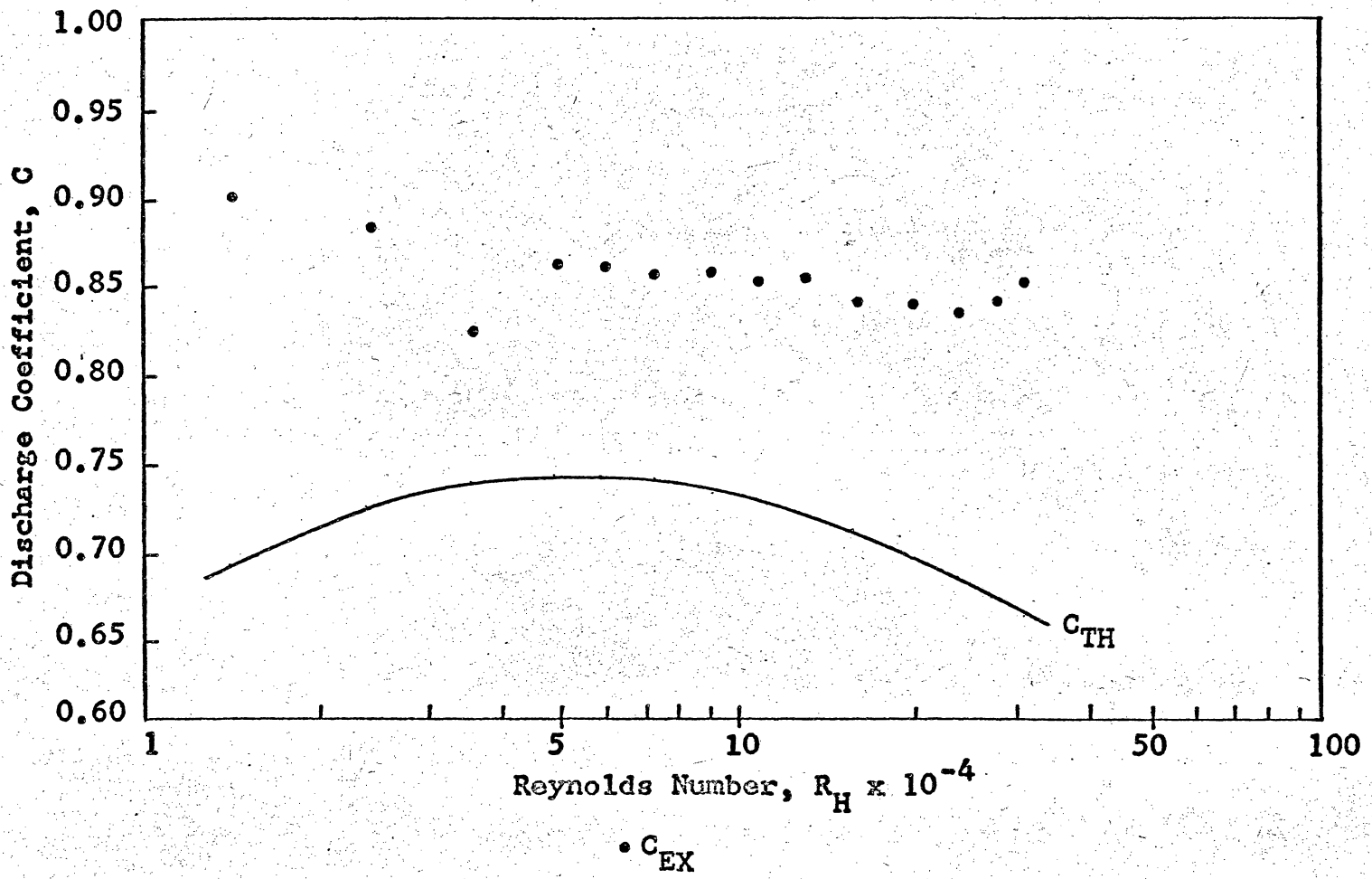

Figure 8. Experimental results of Run 1.

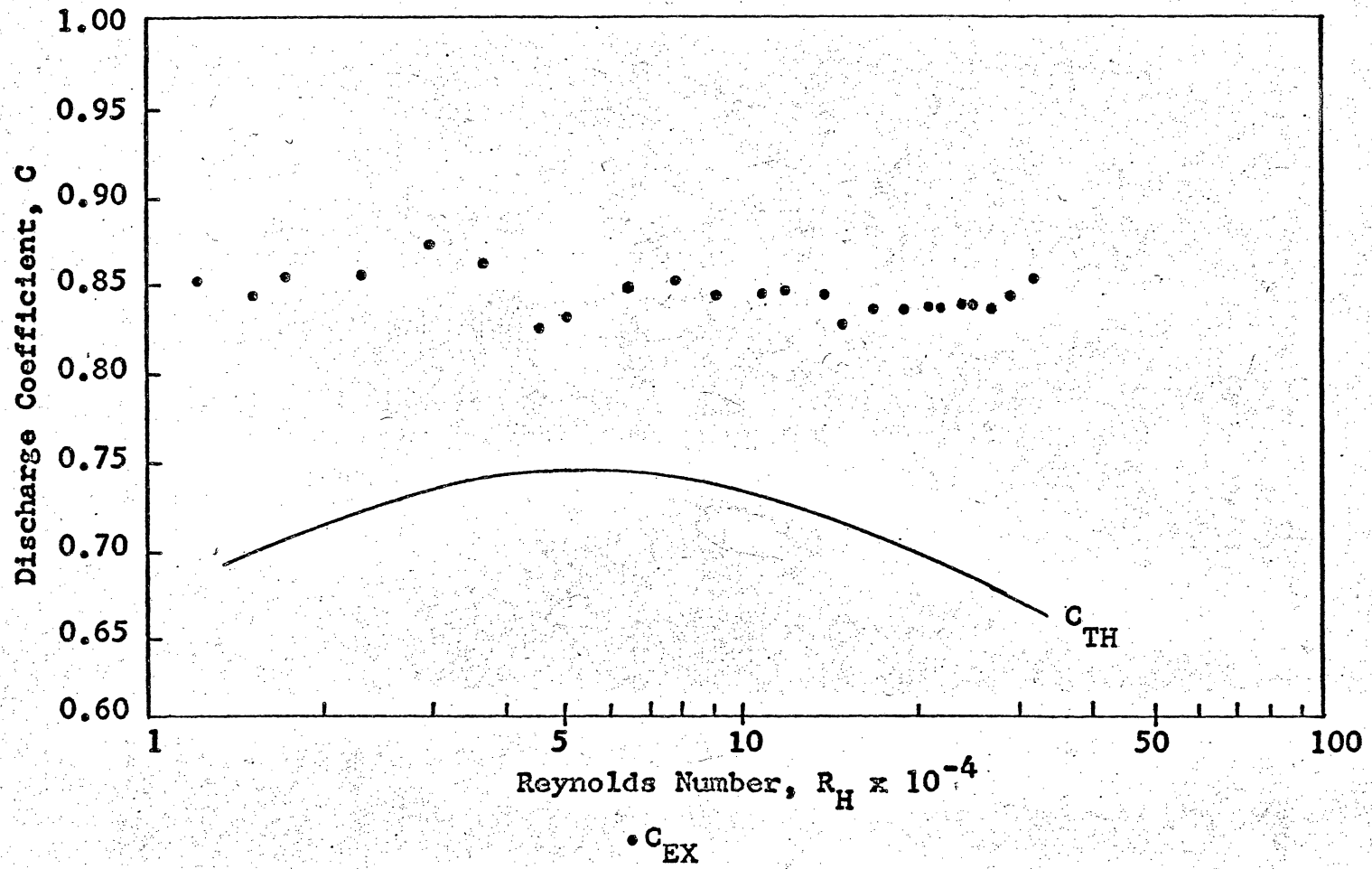

Figure 9. Experimental Results of Run 2.

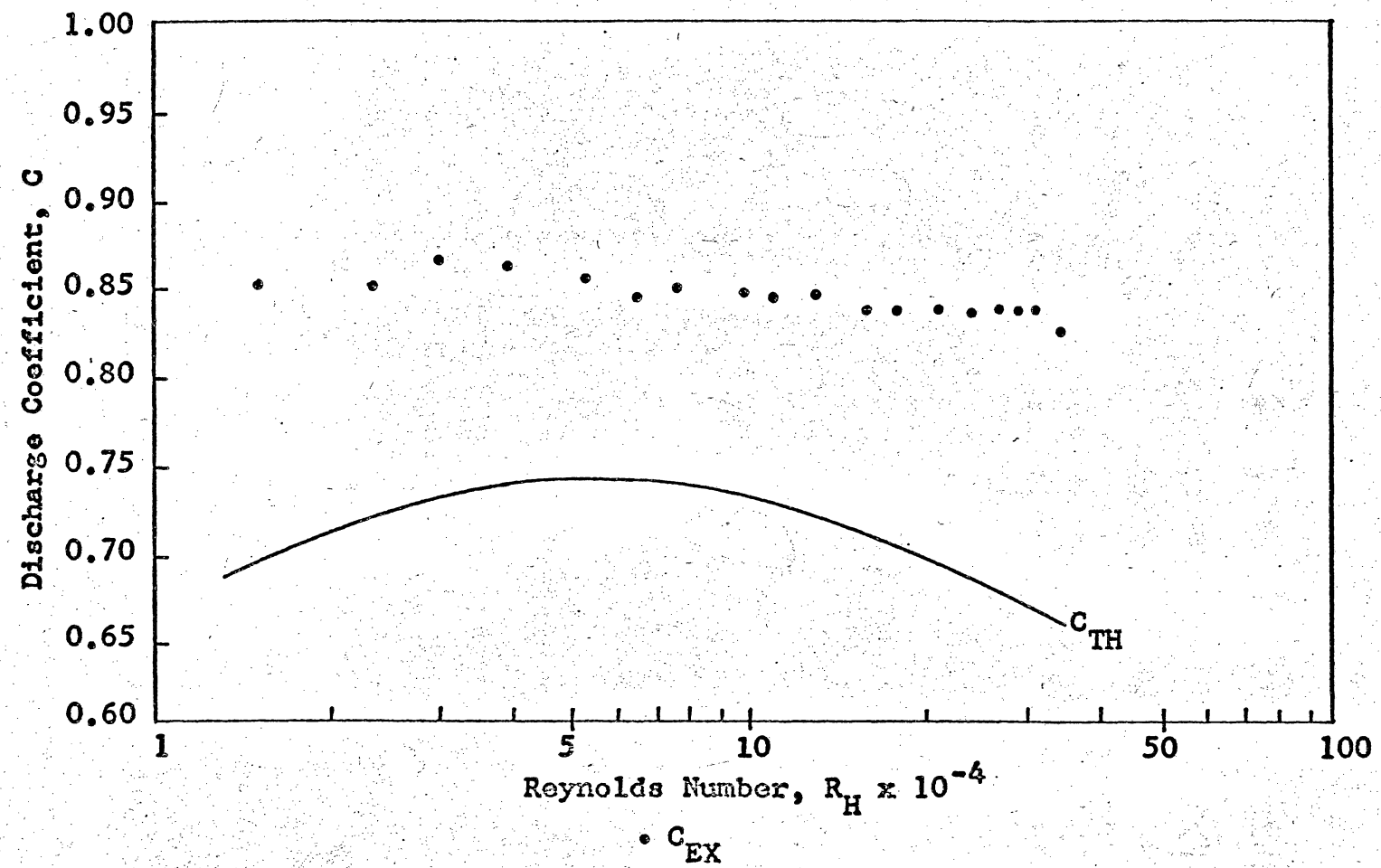

Figure 10. Experimental Results of Run 3.

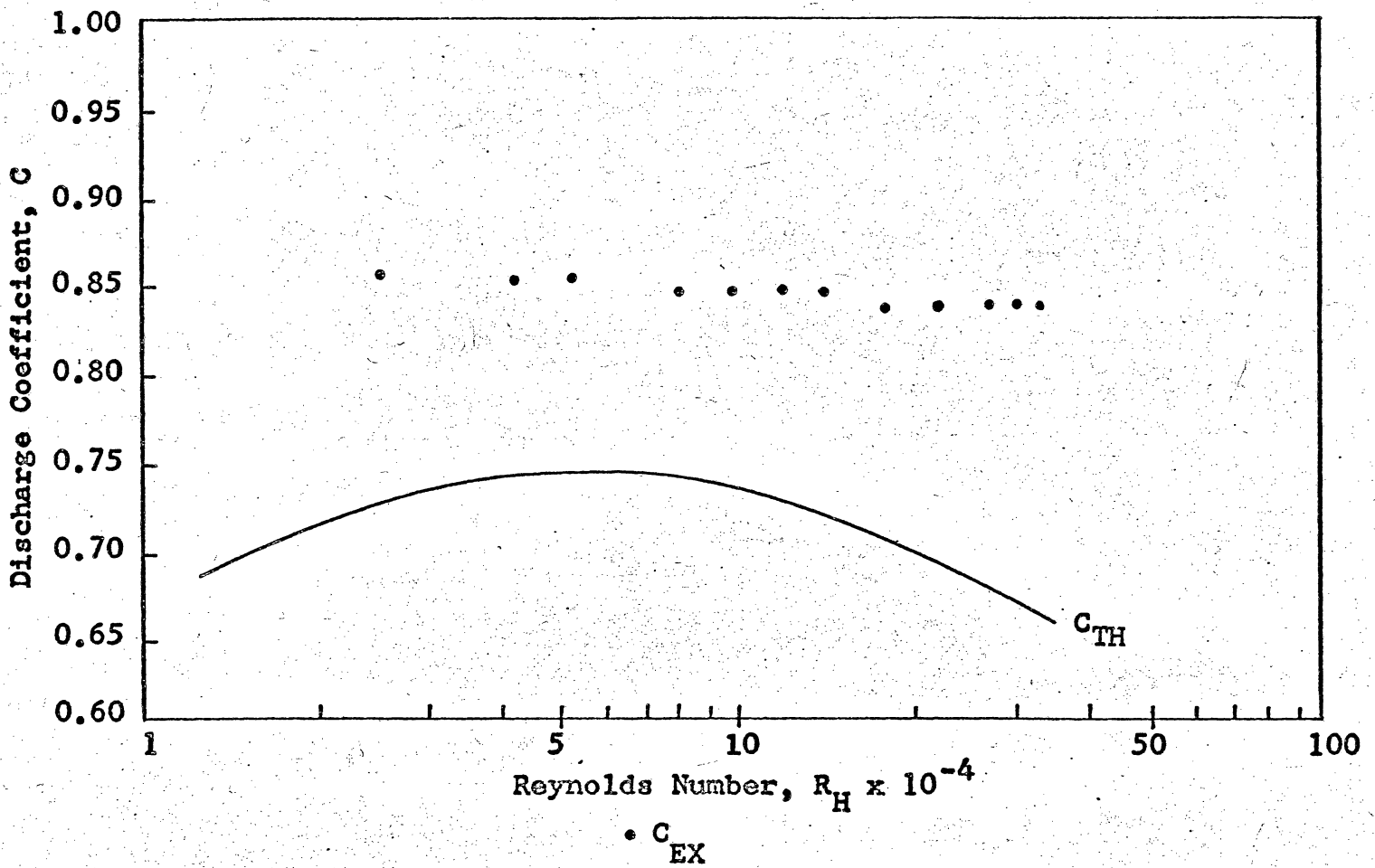

Figure 11. Experimental Results of Run 5.

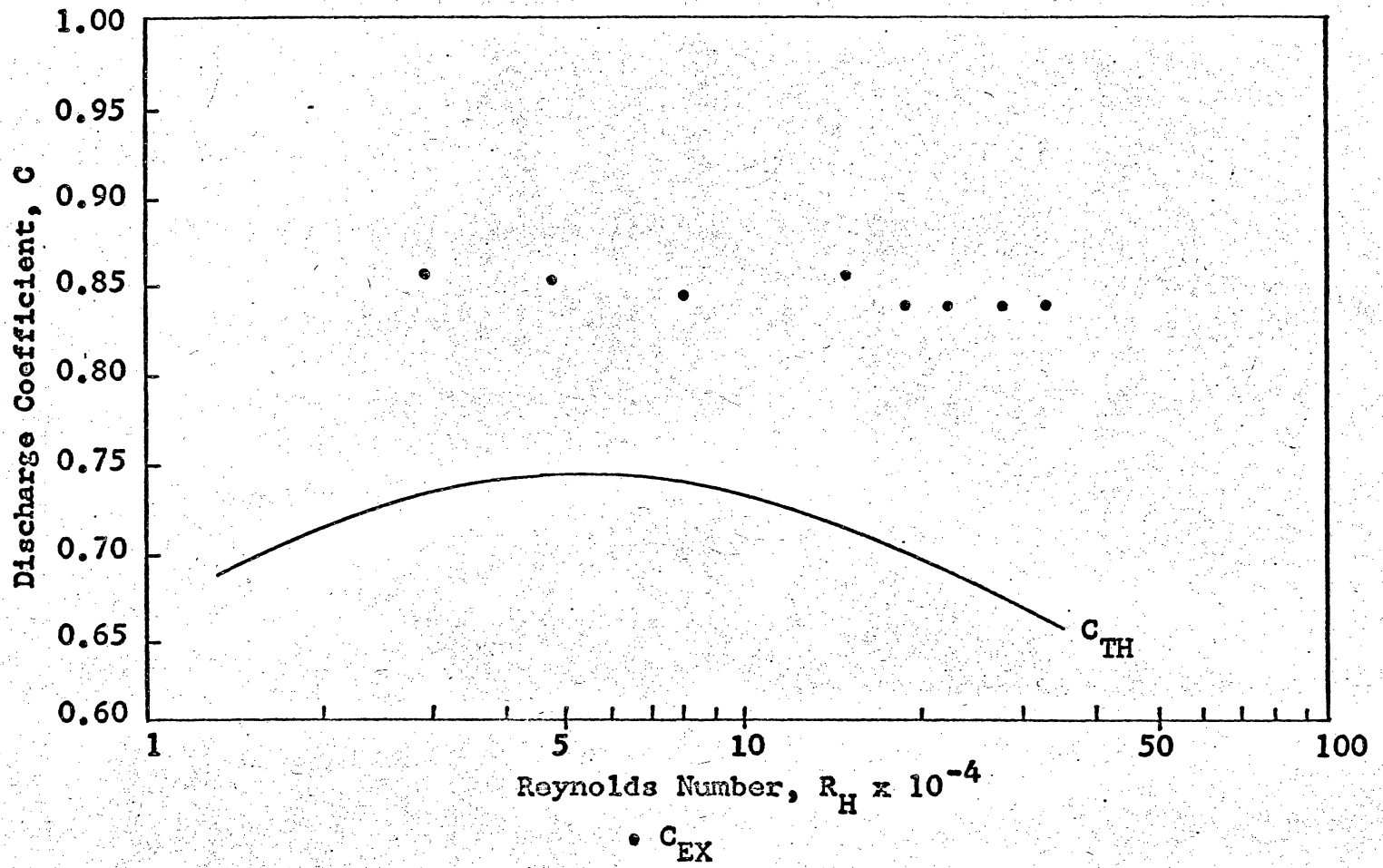

Figure 12. Experimental Results of Run 6.

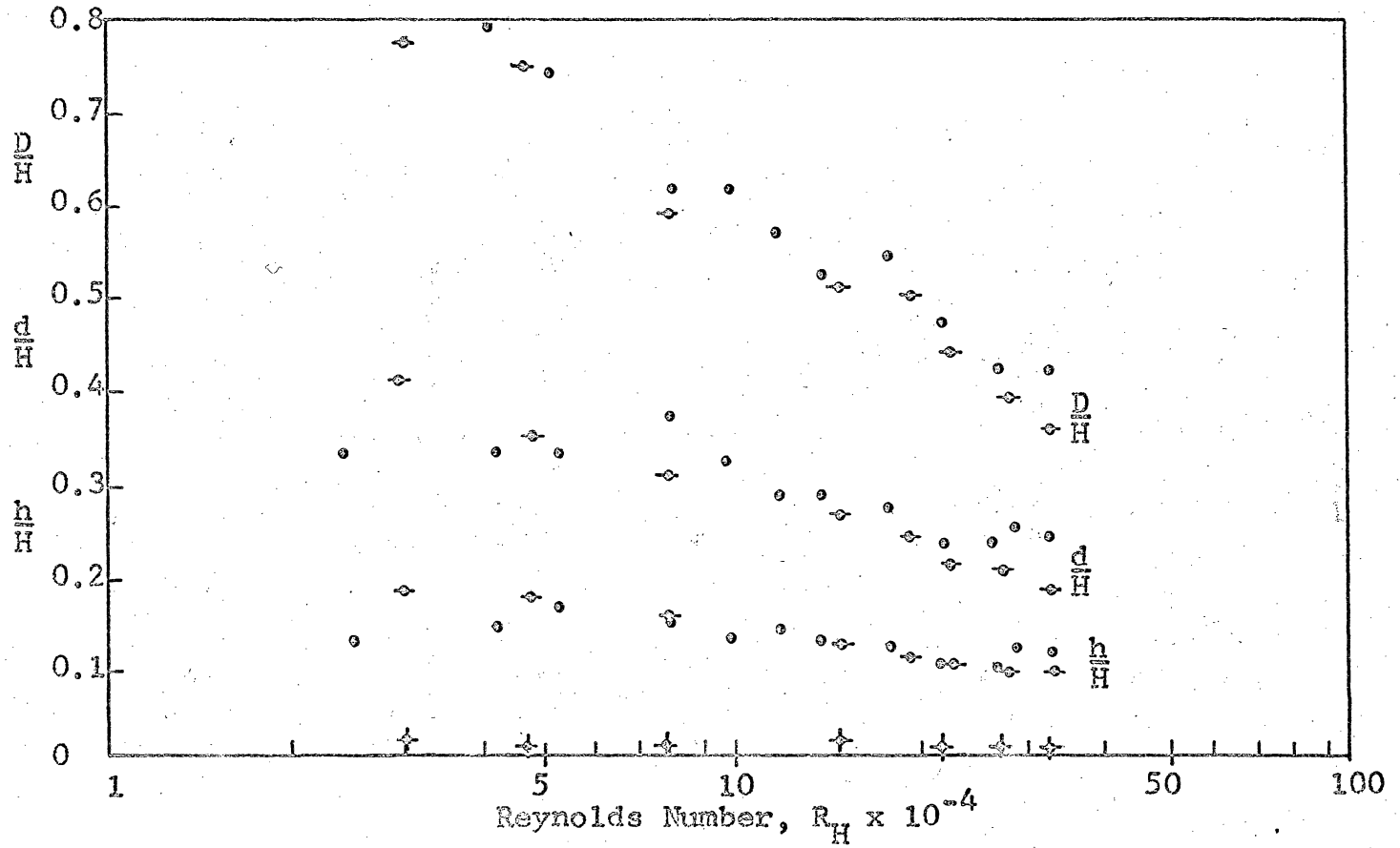

Figure 13. Geometric Ratios $\frac{D}{H}$, $\frac{d}{H}$, and $\frac{h}{H}$ as Functions of Reynolds number.

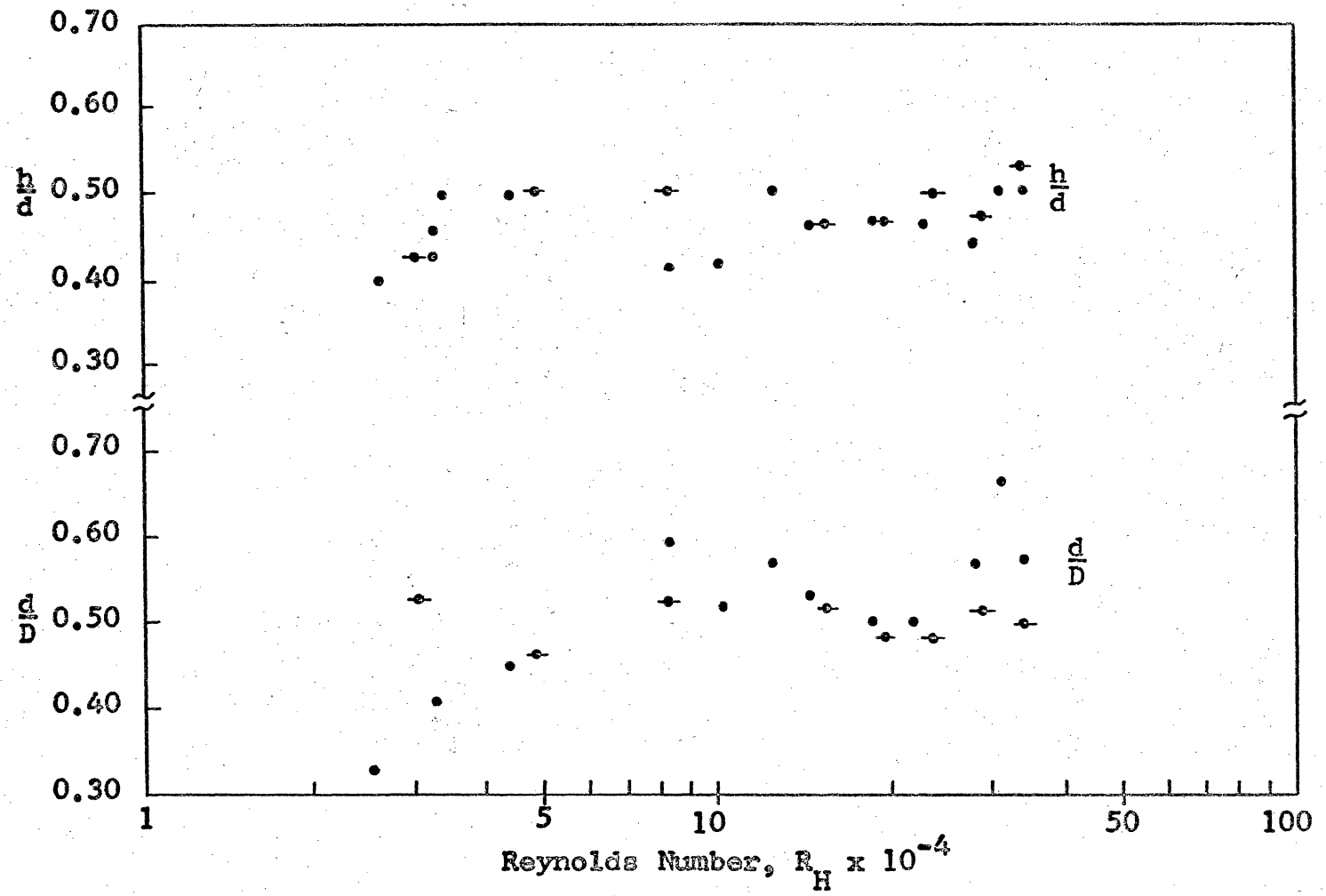

Figure 14. Geometric Ratios $\frac{d}{D}$ and $\frac{h}{d}$ as Functions of Reynolds Number R_H.

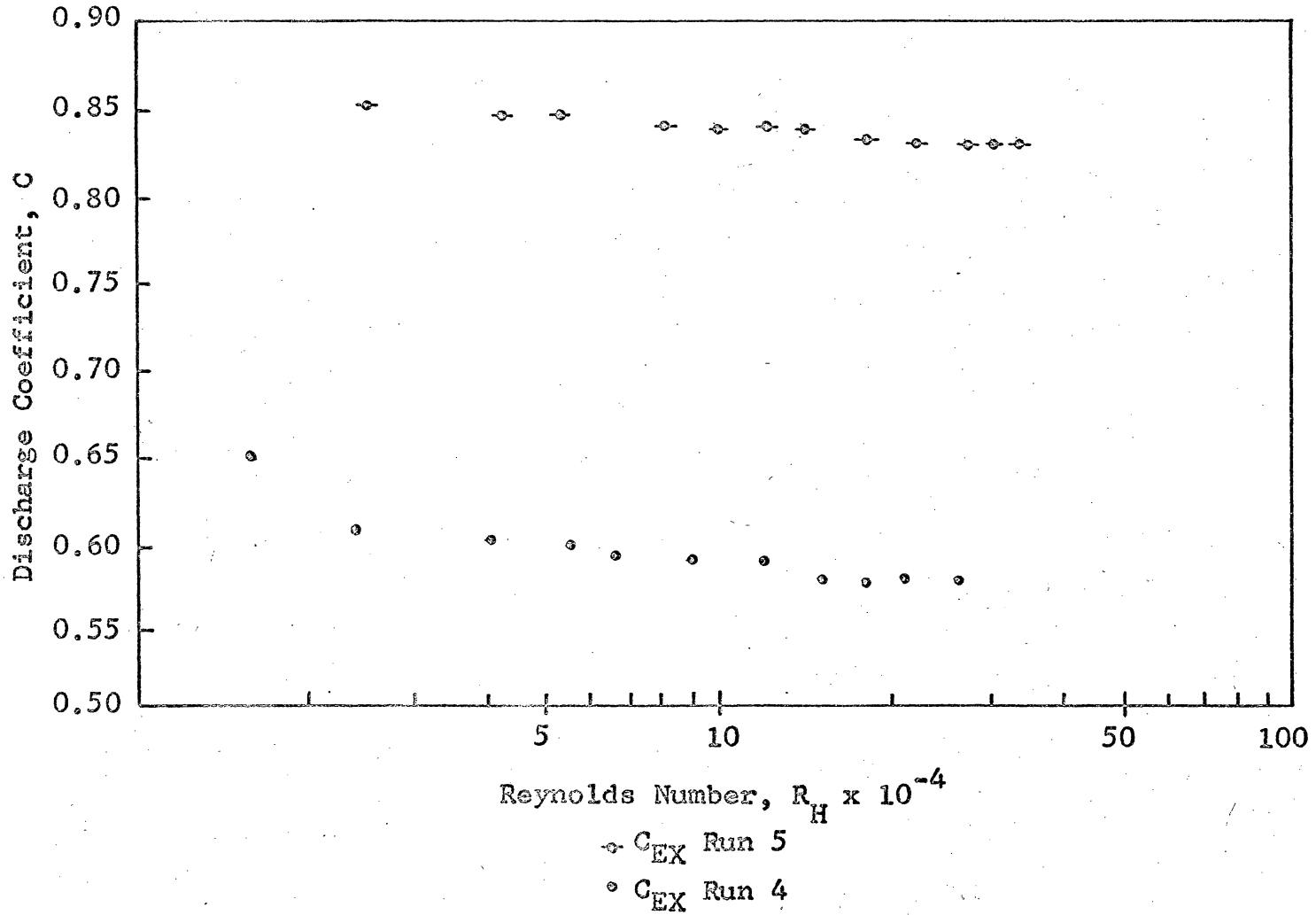

Figure 15. Experimental Results of Runs 4 and 5.

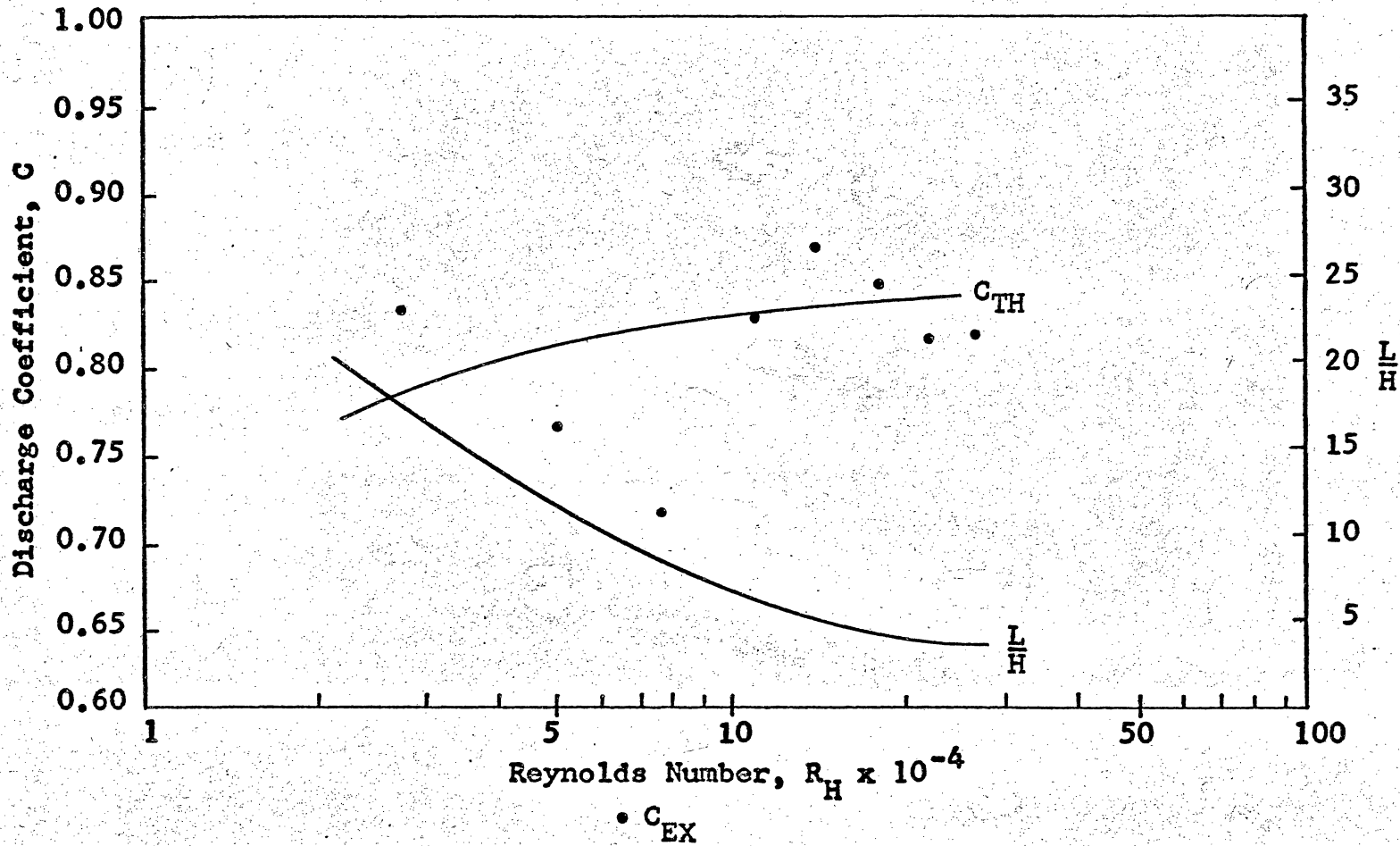

Figure 16. Results of Blackwell's Experiments, Weir 10.

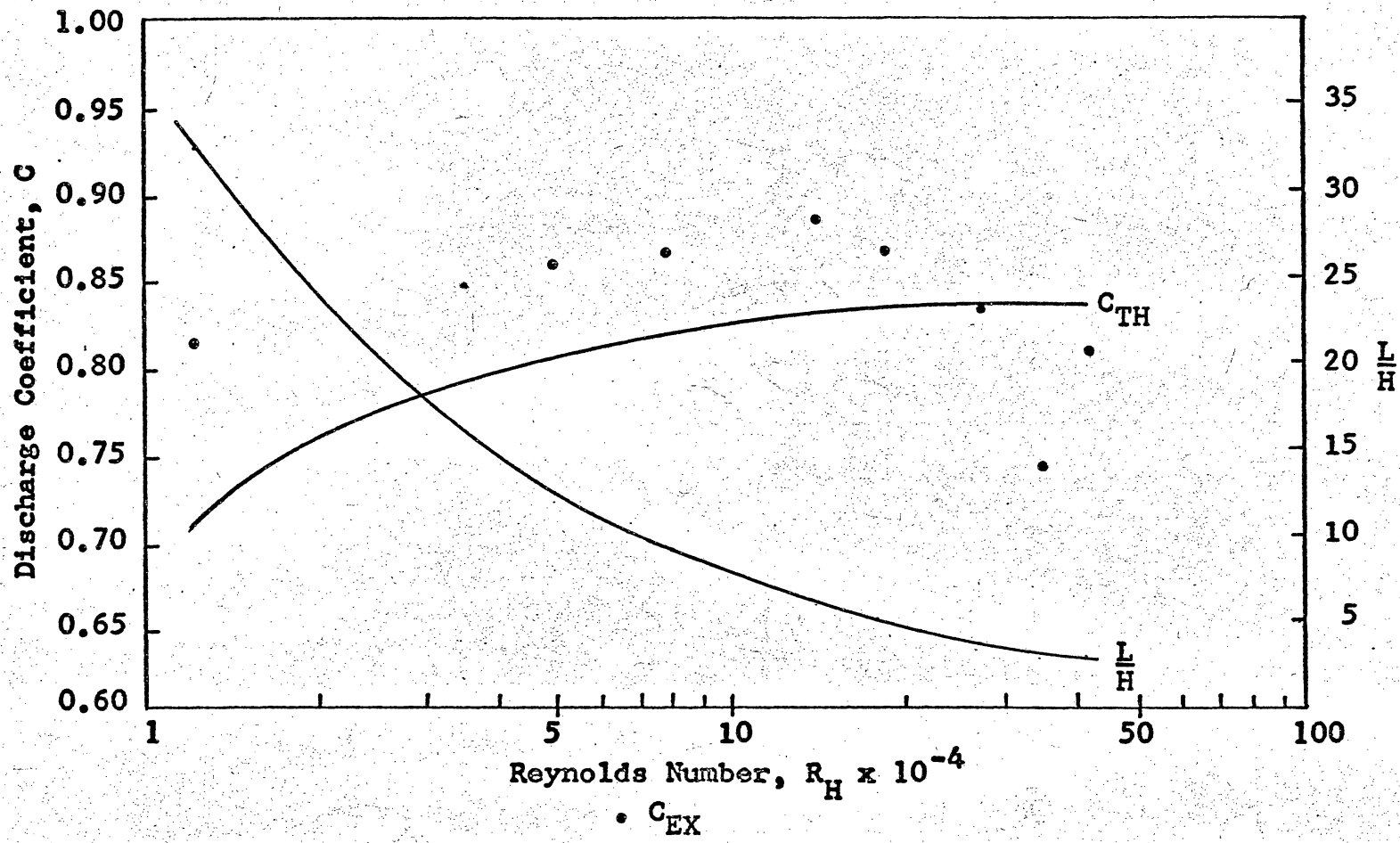

Figure 17. Results of Blackwell's Experiments, Weir 11.

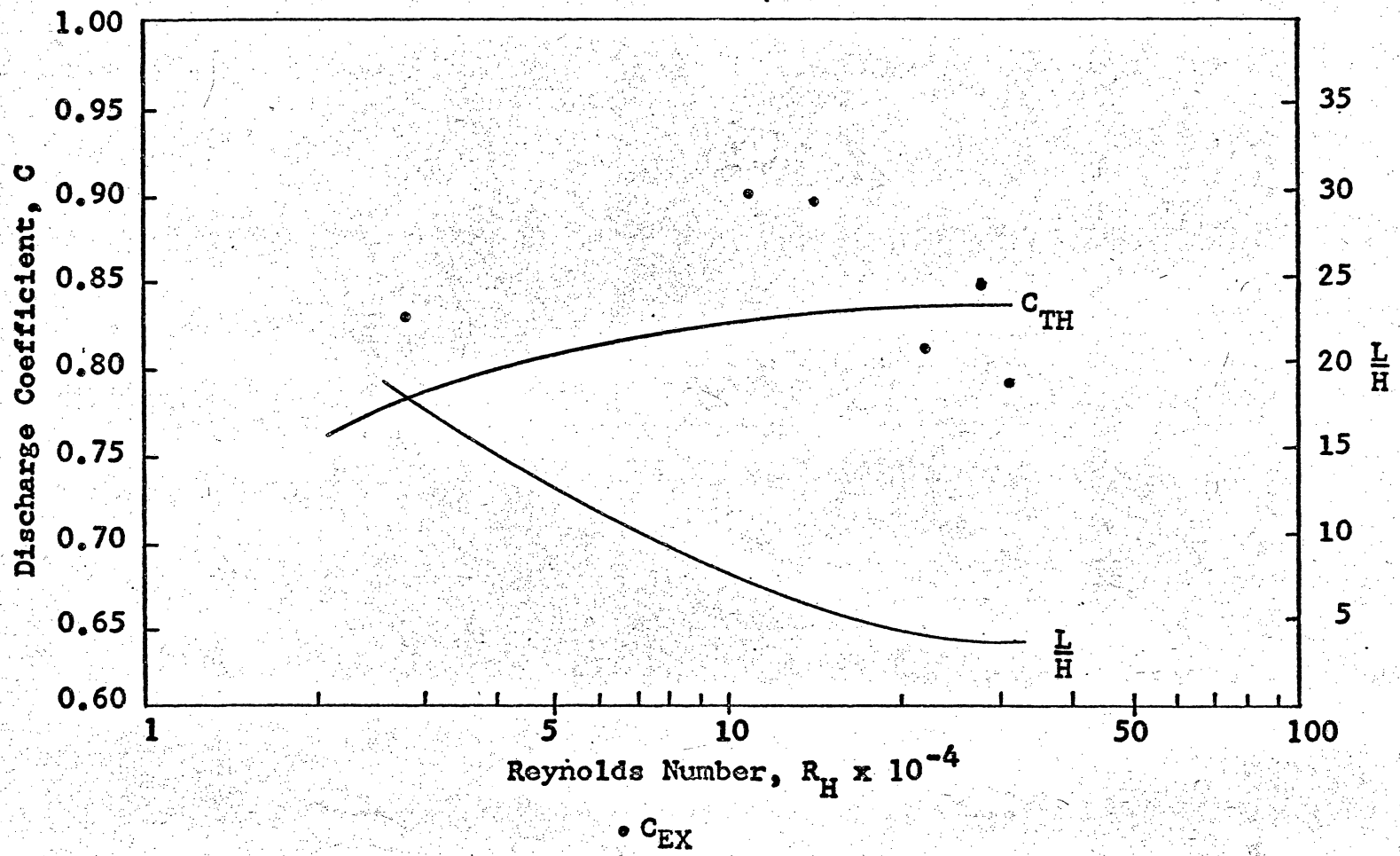

Figure 18. Results of Blackwell's Experiments, Weir 12.

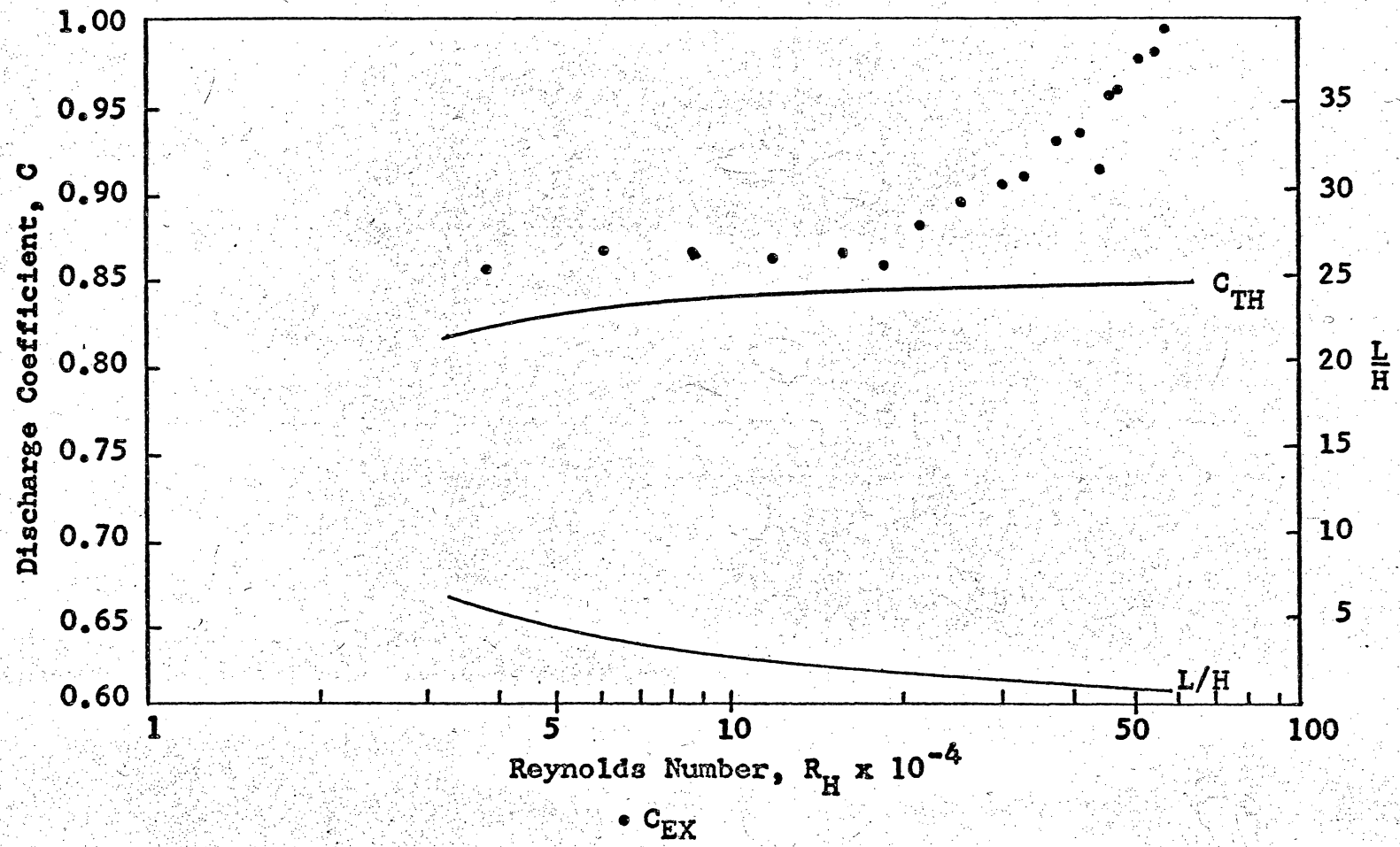

Figure 19. Results of Bazin's Experiments, Series 113.

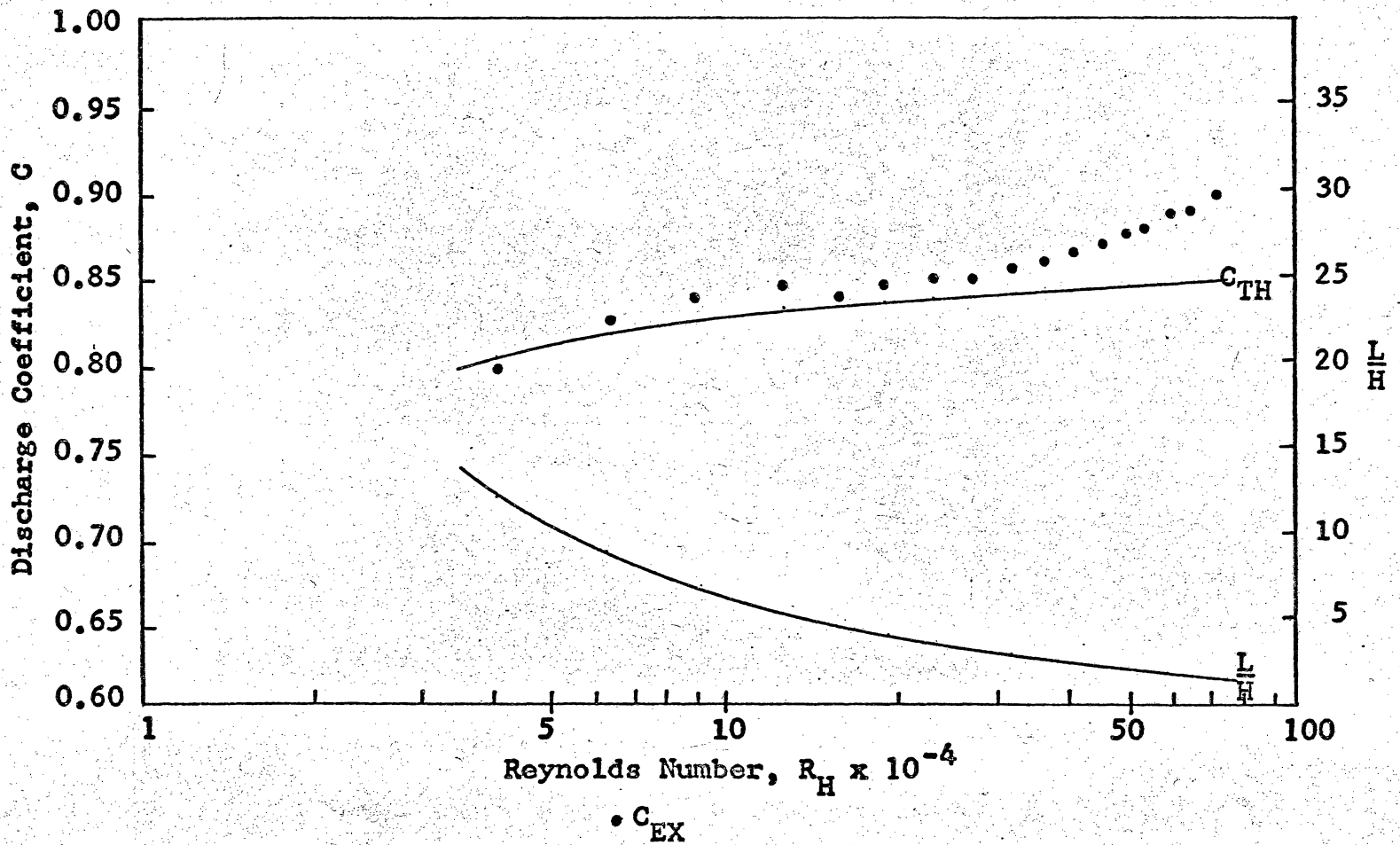

Figure 20. Results of Bazin's Experiments, Series 114.

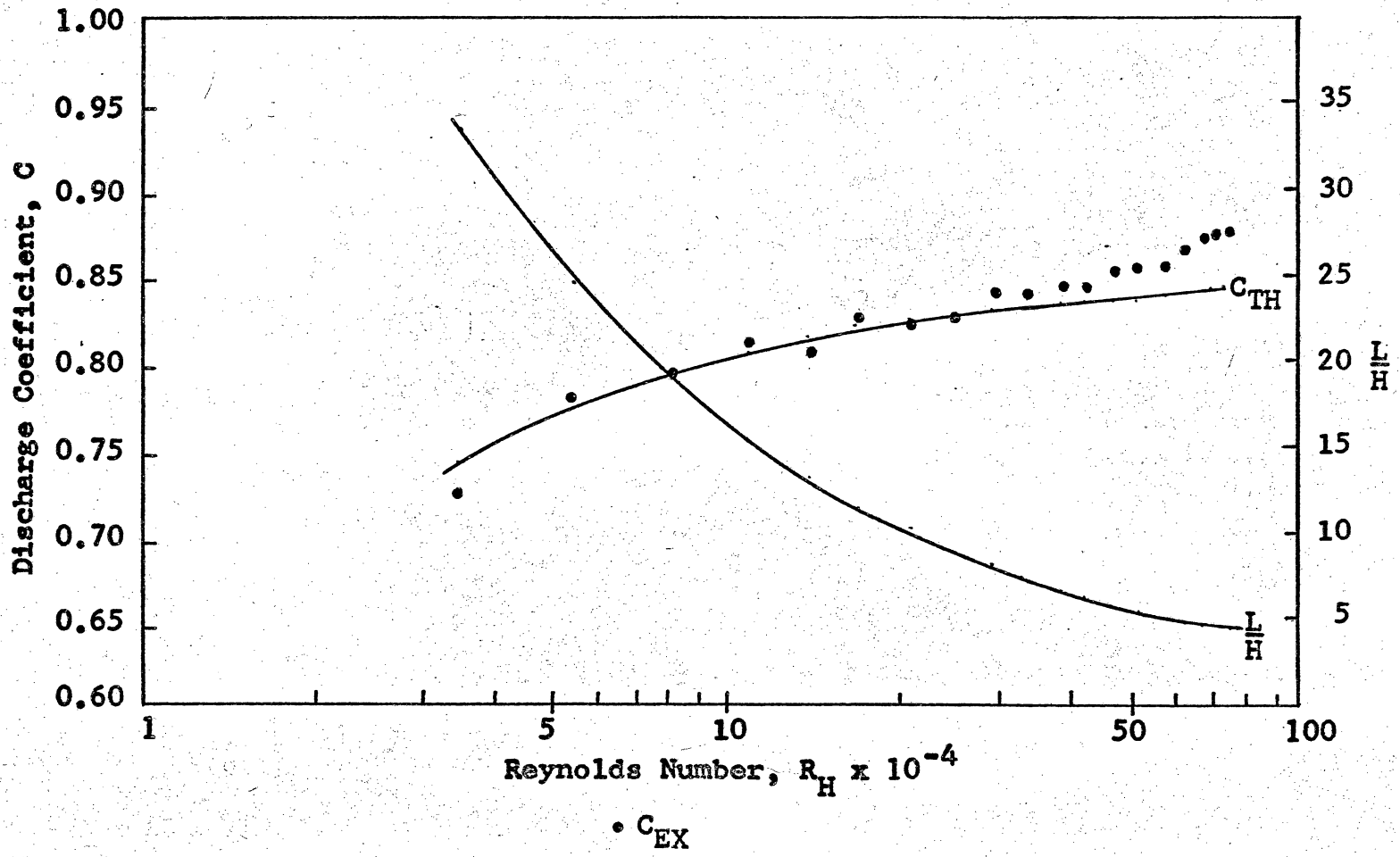

Figure 21. Results of Bazin's Experiments, Series 115.

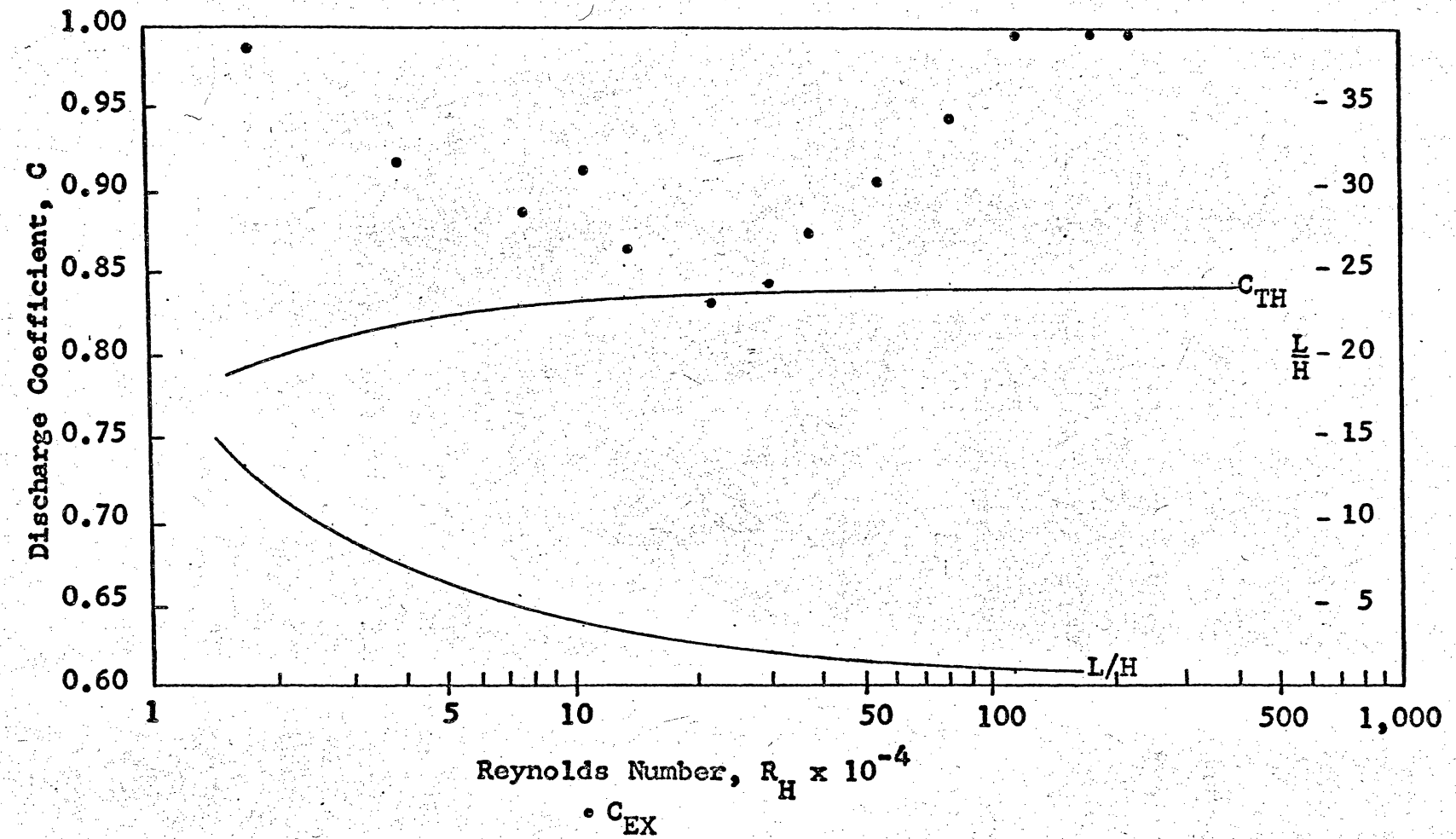

Figure 22. Results of Horton's U.S.G.S. Tests, Series 41.

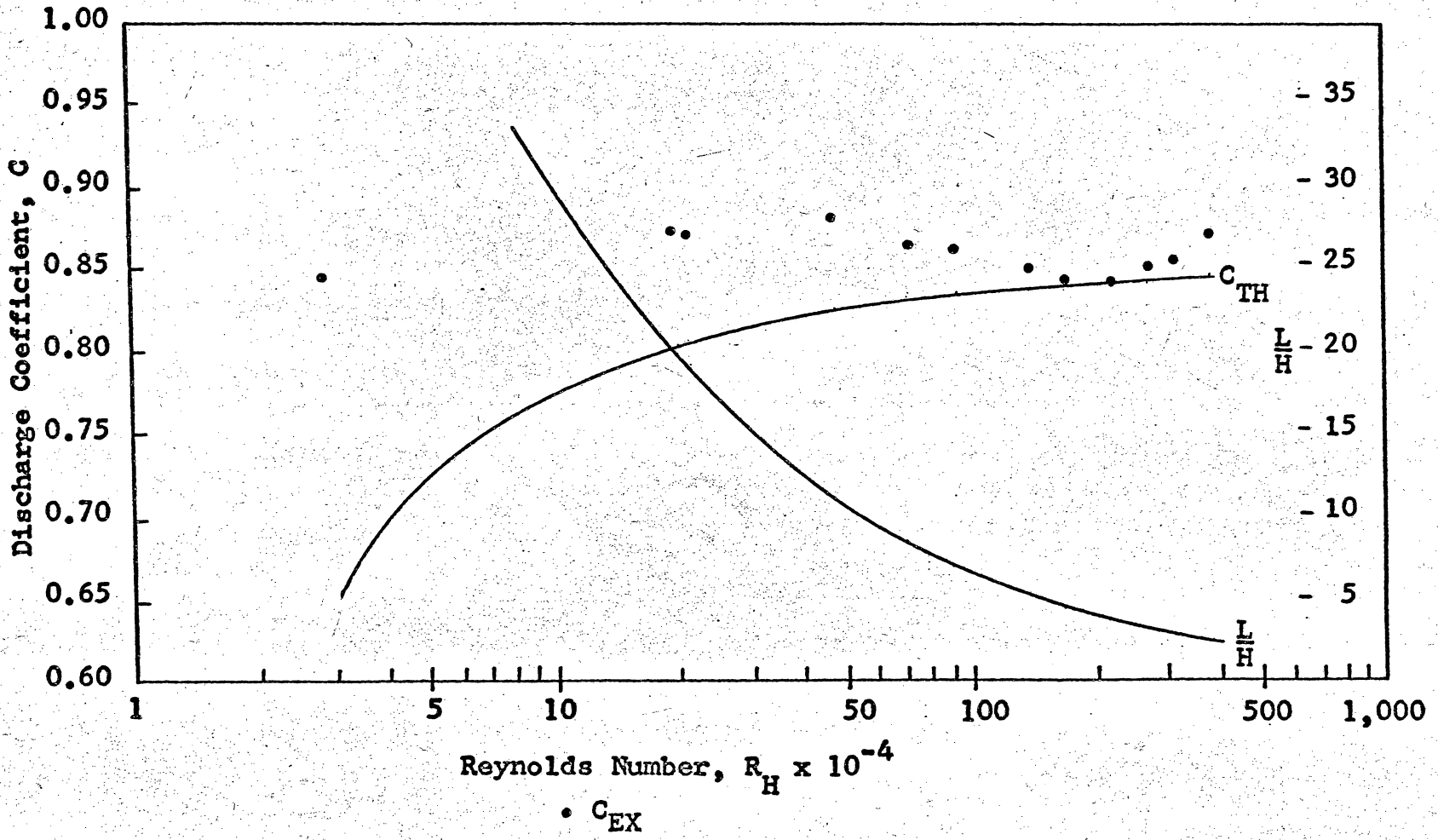

Figure 23. Results of Horton's U.S.G.S. Tests, Series 42.

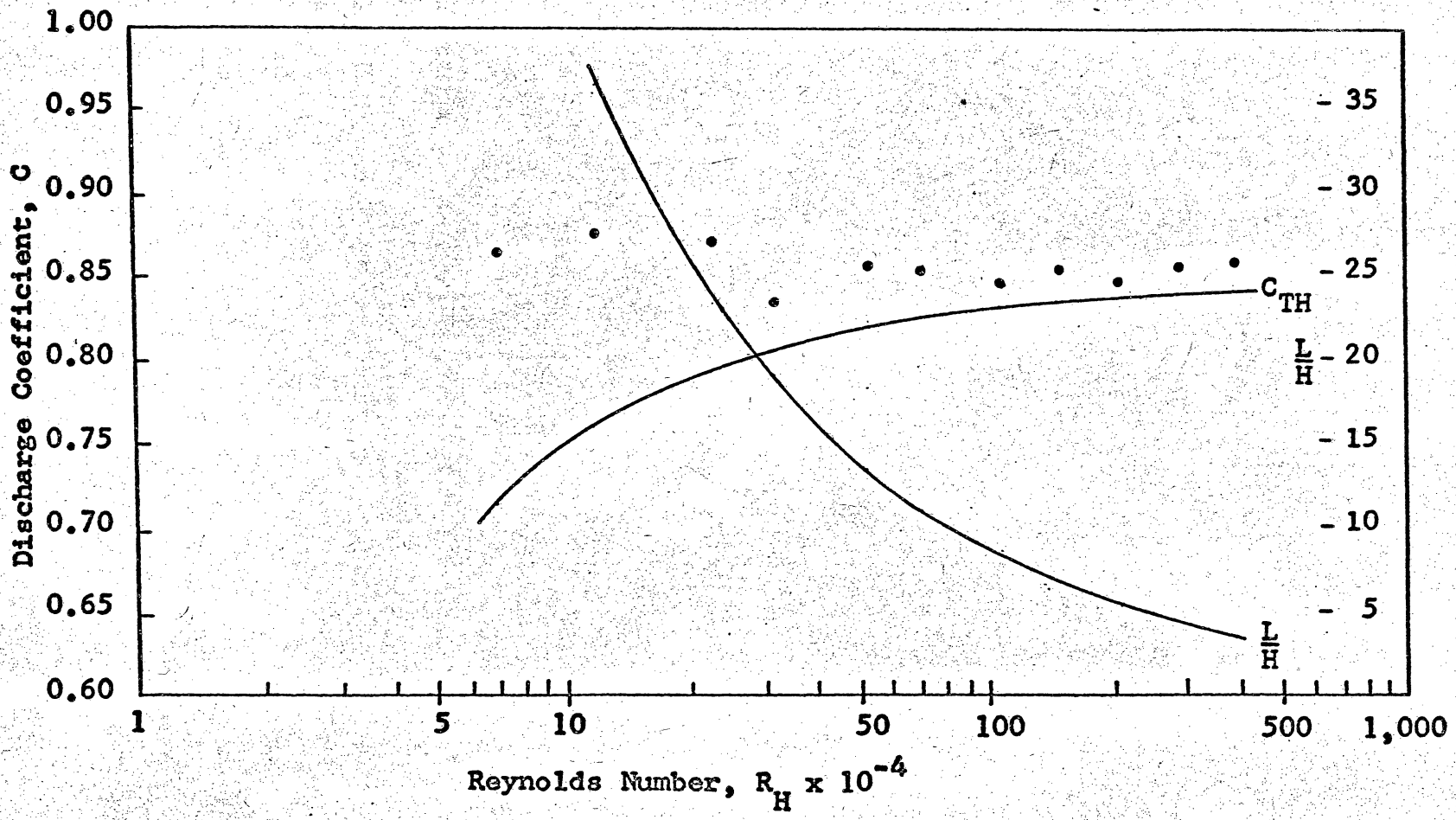

Figure 24. Results of Horton's U.S.G.S. Tests, Series 43.

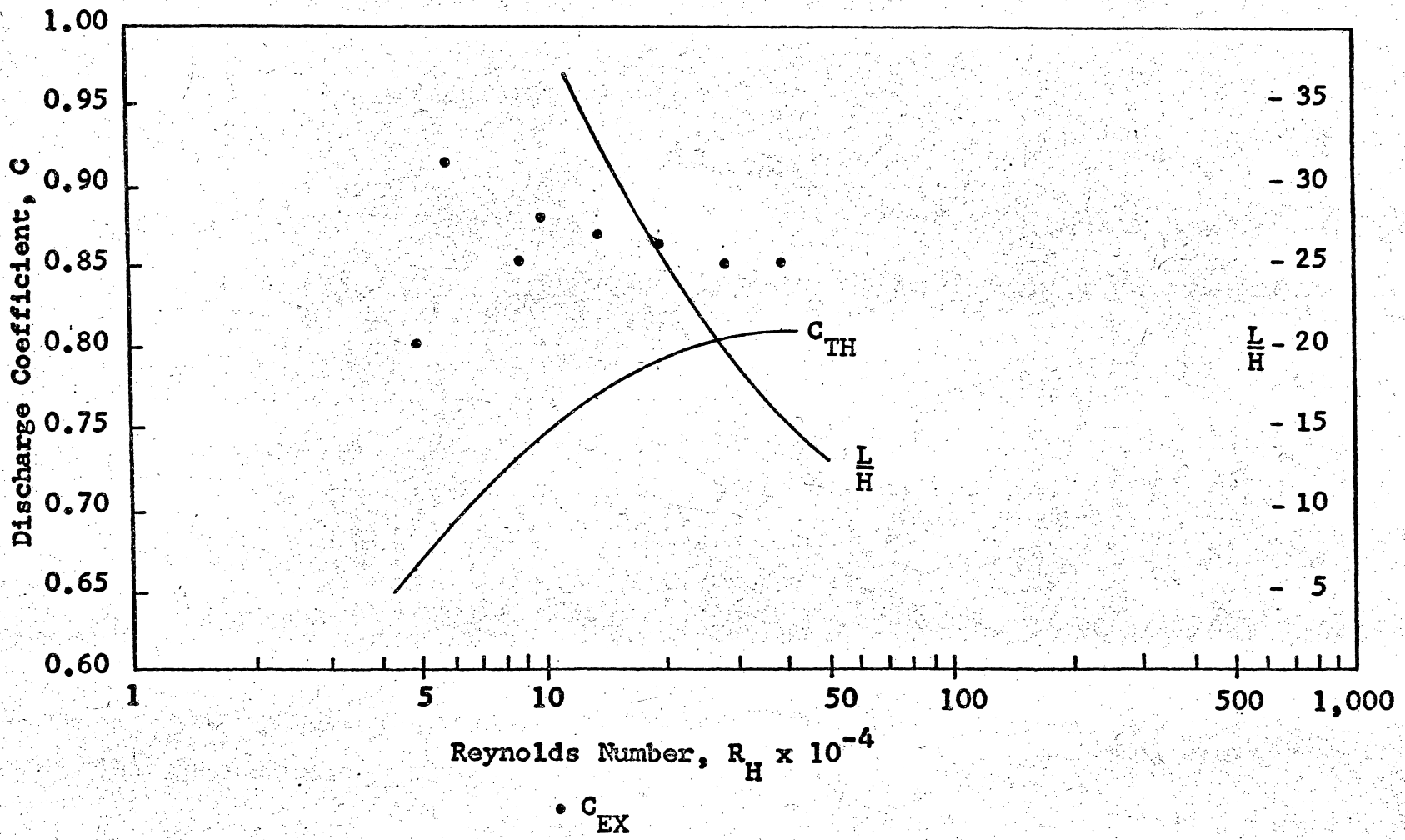

Figure 25. Results of Horton's U.S.G.S. Tests, Series 43a.

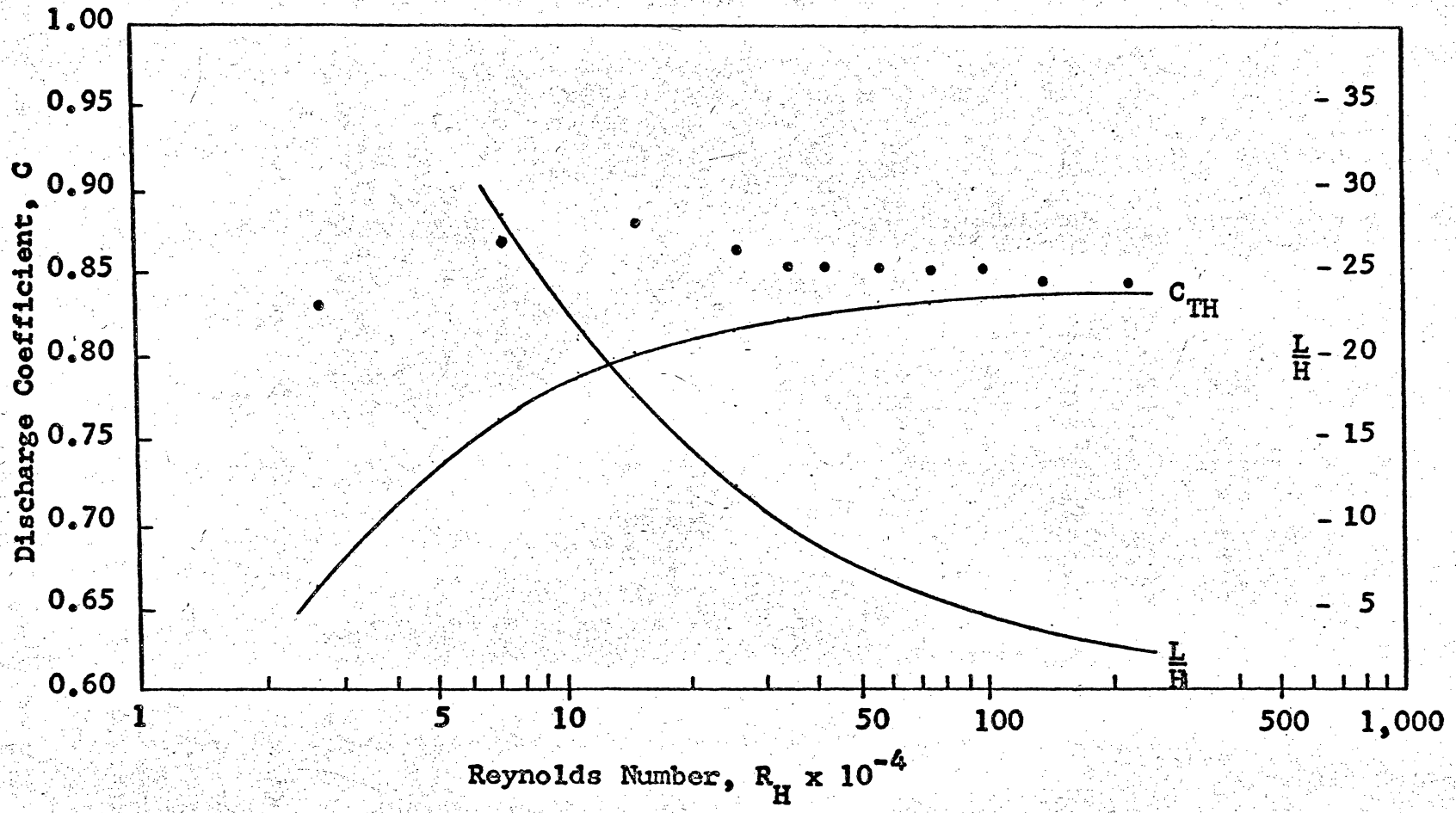

Figure 26. Results of Horton's U.S.G.S. Tests, Series 44.

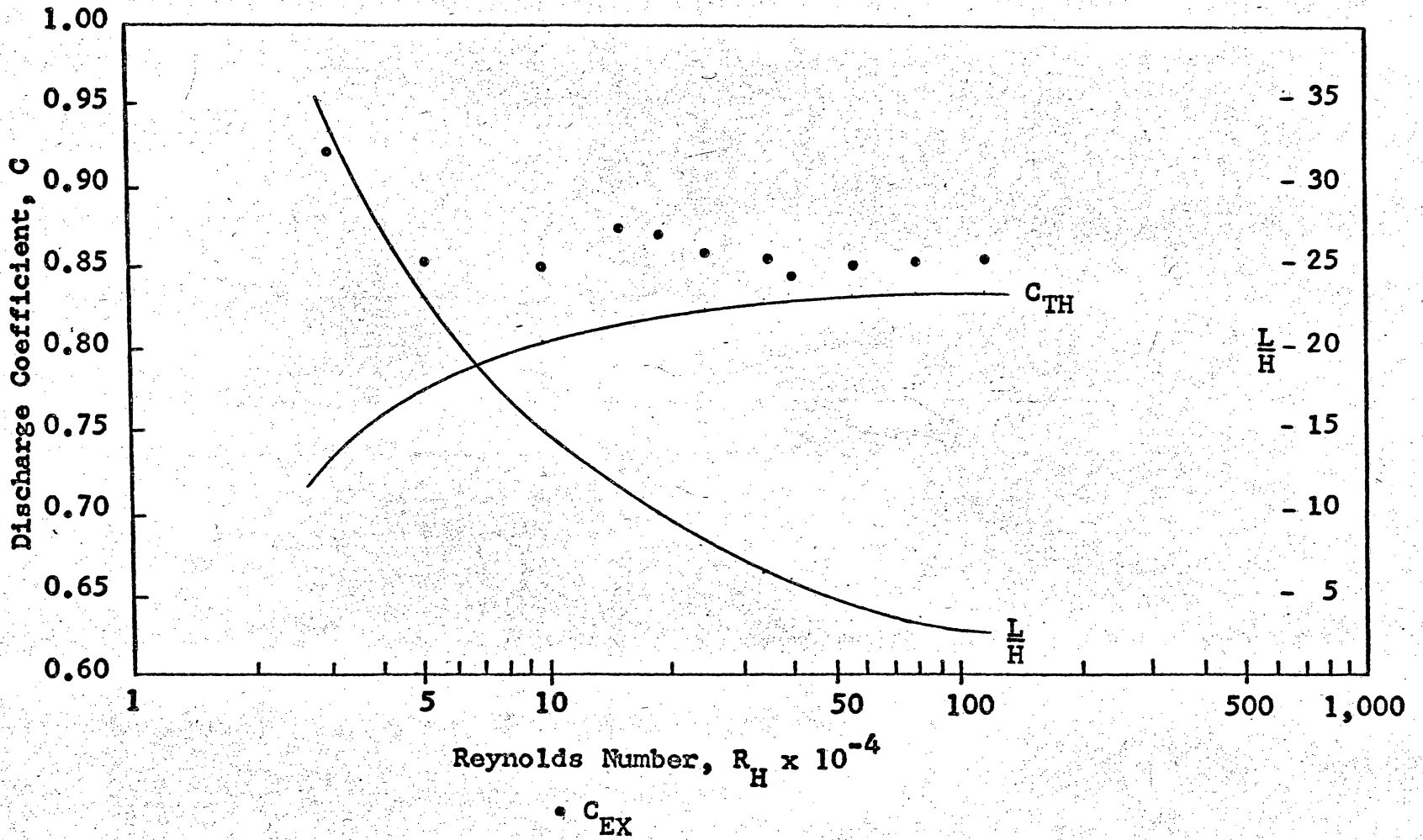

Figure 27. Results of Horton's U.S.G.S. Tests, Series 45.

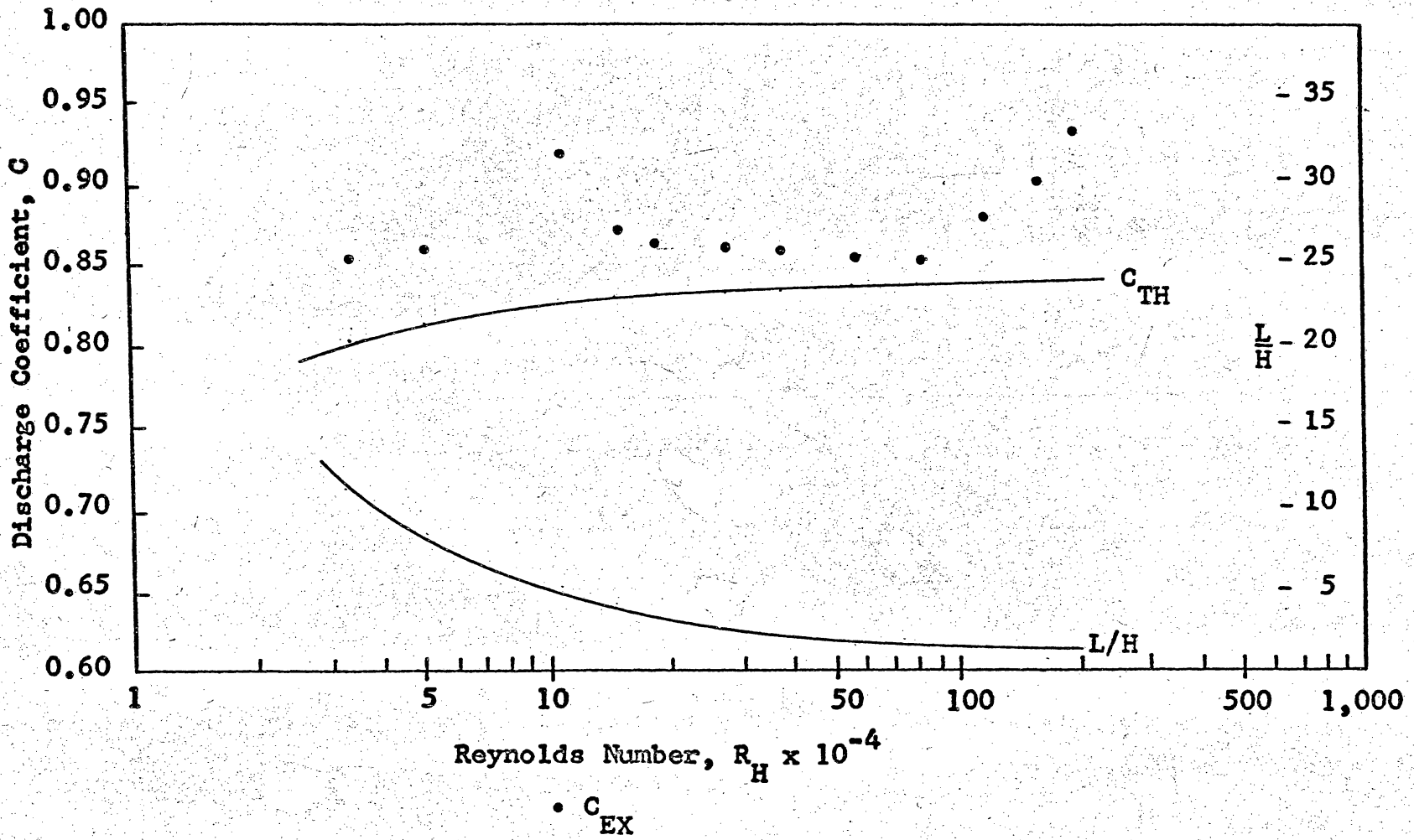

Figure 28. Results of Horton's U.S.G.S. Tests, Series 46.

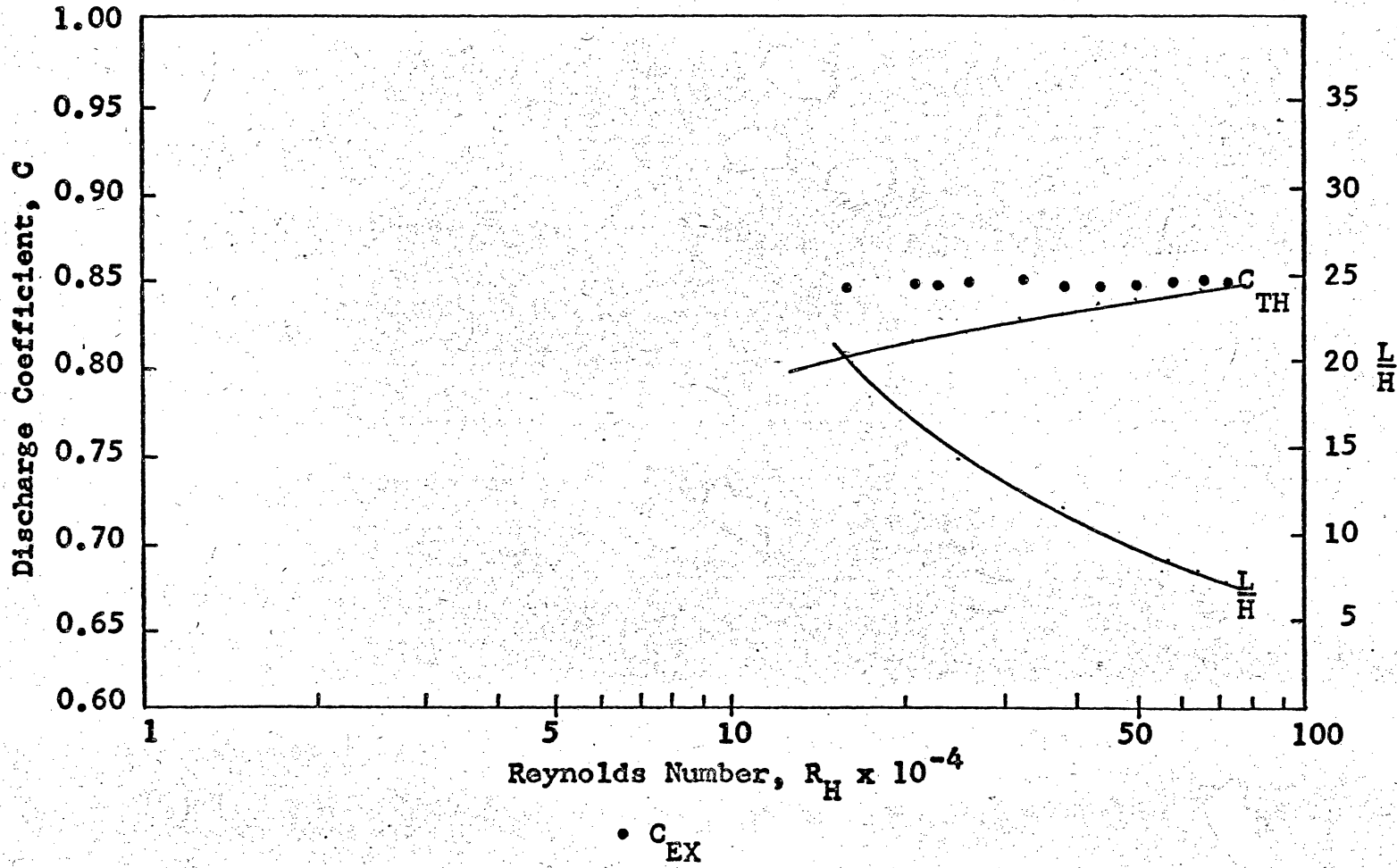

Figure 29. Results of Woodburn's Experiments, Series A.

VI DISCUSSION

Discussion of Experimental Results

Comparison of the experimental discharge coefficients C_{EX} with the theoretical coefficients C_{TH} of Runs 1, 2, 3, 5, and 6 (Figs. 8-12) indicates that Hall's analysis applied to broad-crested weirs of finite crest width produces values of the discharge coefficient C which are 13 to 21 per cent below the experimental values. The results also indicate that the coefficient C_{EX} is nearly independent of the Reynolds number R_H, decreasing from approximately 0.855 to 0.840 as R_H increases from 25,000 to 300,000. When plotted as a function of log R_H, the rate of decrease of C_{EX} appears to be constant as R_H increases.

The results of the dye studies of the crest separation zone as shown in Fig. 13 indicate that the ratio $\frac{h}{H}$ of the height h of the separation zone to the total head H does not remain constant in the range of Reynolds numbers encountered, as assumed by Hall. The ratio $\frac{h}{H}$ at the crest centerline decreases from approximately 0.15 to 0.11 as the Reynolds number increases from 30,000 to 330,000, while the theory assumes the ratio $\frac{h}{H}$ to have a constant magnitude of 0.109. At a distance of one inch from the side wall, $\frac{h}{H}$ remains nearly constant at 0.010, or approximately one tenth of the assumed magnitude (Fig 13). It was observed that the height

h of the separation zone decreased linearly from the centerline of the weir crest to the side wall.

Figure 13 also shows that the ratio $\frac{d}{H}$, indicating the location of the maximum separation height, does not have a constant value of 0.25 as assumed by the analysis, but decreases from approximately 0.35 to 0.25 as the Reynolds number R_H increases from 30,000 to 330,000.

The experimental results (Fig. 13) also show that the ratio $\frac{D}{H}$ of the reattachment distance D to the total head H does not have the constant magnitude of 1.0 as assumed by Hall, but decreases from approximately 0.7 to 0.4 as the Reynolds number increases from 50,000 to 350,000.

Figure 14 indicates that the geometric proportions of the separation zone given by the ratios $\frac{h}{D}$ and $\frac{d}{D}$ are nearly constant, increasing slightly with increasing Reynolds number.

The results of Run 4 (Fig. 15) show that the experimental discharge coefficient C_{EX} for the sharp-crested rectangular weir is nearly independent of the Reynolds number, decreasing slightly as R_H increases in a manner similar to that for the broad-crested experimental weir.

The distances d and D were measured only on the weir crest centerline due to the difficulty of observation near the side walls. An attempt to measure the geometry of the wall separation zone was unsucessful because of the air

entrainment at the free surface and the resulting difficulty of observation.

It was noted qualitatively that the separation zones on the side walls consisted of aerated regions extending down the wall from the free surface to a depth of approximately $\frac{H}{2}$. The maximum thickness of the separation zones diminished from the free surface downward toward the weir crest.

The occurrence of pronounced downward flow at the crest entrance was observed by injecting dye into the flow with a syringe and hypodermic needle. In the vicinity of the wall separation zones, the flow was directed downward at angles of approximately 45° from the horizontal.

A stable standing wave was observed on the weir crest at heads exceeding approximately 0.25 feet. The shape of the wave was not recorded but it was noted that the shape was similar to that recorded by Woodburn for a similar weir (22).

Analysis of Data from the Literature

No data were available from the literature for contracted broad-crested weirs of finite crest widths which would exhibit the wall separation of the three-dimensional weir analyzed by Hall. However, a comparison of the experimental results with the theoretical discharge coefficients

C_{TH} given by Hall's two-dimensional analysis gives an indication of the validity of the two-dimensional theory.

The experimental coefficients given by Blackwell's data (Figs. 16-18) show little consistency but do not appear to contradict Hall's analysis.

Greater consistency is apparent in Bazin's results. Series 113 (Fig. 19) produced experimental coefficients C_{EX} which are 3 to 8 per cent above the theoretical coefficients C_{TH} for Reynolds numbers from 50,000 to 600,000. The theoretical coefficients of Series 114 and 115 (Figs. 20 and 21) agree with the experimental coefficients within 1.0 per cent and tend to support Hall's theory for the two-dimensional case.

Reasonable agreement between theory and experiment is not found in any of Horton's U.S.G.S. results (Figs. 22-28). In all cases, the theory produces discharge coefficients which are from 1 to 18 per cent below the experimental coefficients for Reynolds numbers of 50,000 to 600,000. In some cases, better agreement is found outside the range of Reynolds numbers for which the analysis was assumed to be valid (Series 42, 43, 44, 45).

Woodburn's results (Fig. 29) show agreement within 0.5 to 5 per cent between the theoretical and experimental coefficients for Reynolds numbers from 160,000 to 730,000. It should be noted that Woodburn's suppressed weir had aspect

ratios $\frac{B}{H}$ of 1.4 to 4.0 but the data were reanalyzed using Hall's two-dimensional theory. The effects of taking into account the boundary layers on the walls would be to lower the theoretical coefficients and to reduce the correlation between the theory and experiment.

General Discussion

The experimental results of Runs 1, 2, 3, 5, and 6 show that Hall's analysis of the discharge coefficient for a three-dimensional broad-crested weir fails to produce coefficients that agree with experimental results.

The analysis of data from the literature indicates that Hall's analysis does not produce values of the discharge coefficient which are in consistent agreement with experimental results for the two-dimensional case.

The failure of the theory to predict the correct coefficients is due partly to the invalidity of the assumptions made regarding the geometry of the crest separation zones as shown in Figs. 13 and 14.

The simplified flow model for the three-dimensional broad-crested weir also does not account for the interaction of the separated side wall flow with the crest flow. The effect of the interaction is to alter the separation pattern on the crest by reducing the height of the separation zone near the side walls and probably to suppress the initial

development of the crest boundary layer in the vicinity of the walls. Interaction of this nature would tend to increase the unit discharge near the walls and would therefore increase the actual discharge coefficient of the weir as compared to that given by Hall's theory.

The extension of Hall's theory to the three-dimensional case is invalid since it was assumed that the side wall separation was identical to the separation on the weir crest and thus had a constant separation thickness of 0.109H. The separation thickness on the side walls varies with the height above the weir crest, causing the effective crest width B_{eff} to vary in a similar manner.

The data of Runs 5 and 6 were reanalyzed to determine the dependence of the theoretical coefficient C_{TH} on the height of the separation zone. It was found that in order to obtain reasonable agreement between the experiments and Hall's theory for the three-dimensional weir, it was necessary to assume that the maximum separation height h had a magnitude of 0.05H instead of 0.109H.

It therefore appears that the flow model analyzed by Hall is oversimplified due to its assumptions regarding the shape of the separation zone.

The model also assumes that critical flow occurs at the downstream end of the weir crest, since this is the point at which the boundary layer displacement thickness is

evaluated. However it is questionable whether the location of critical flow is always at the downstream end of the weir. This would clearly be true for the case of large values of the ratio $\frac{L}{H}$ where boundary friction on the weir crest would require subcritical flow to exist on the crest with critical flow at the free overfall.

For small values of $\frac{L}{H}$, critical flow would occur at the upstream end of the weir, with the limiting case being a sharp-crested weir. For intermediate values of $\frac{L}{H}$ such as those encountered with broad-crested weirs, the location of critical flow may be expected to vary between the limits of the long-crested weir and the sharp-crested weir.

The similarity between the behavior of the experimental coefficients for the sharp- and broad-crested weirs tested indicates that the factor controlling the location of critical flow may be the same in both cases. This would require that the location of the maximum height of the separation zone on the broad-crested weir also be the location of critical flow.

The existence of pronounced downward flow at the crest entrance implies that the initial growth of the crest boundary layer would be retarded and that the initial displacement thickness would be smaller than the height of the separation zone. Thus for sufficiently short crest lengths L, the boundary layer displacement thickness would not

approach the separation height in magnitude and would not function to cause critical flow to occur downstream of the separation region (Fig. 30).

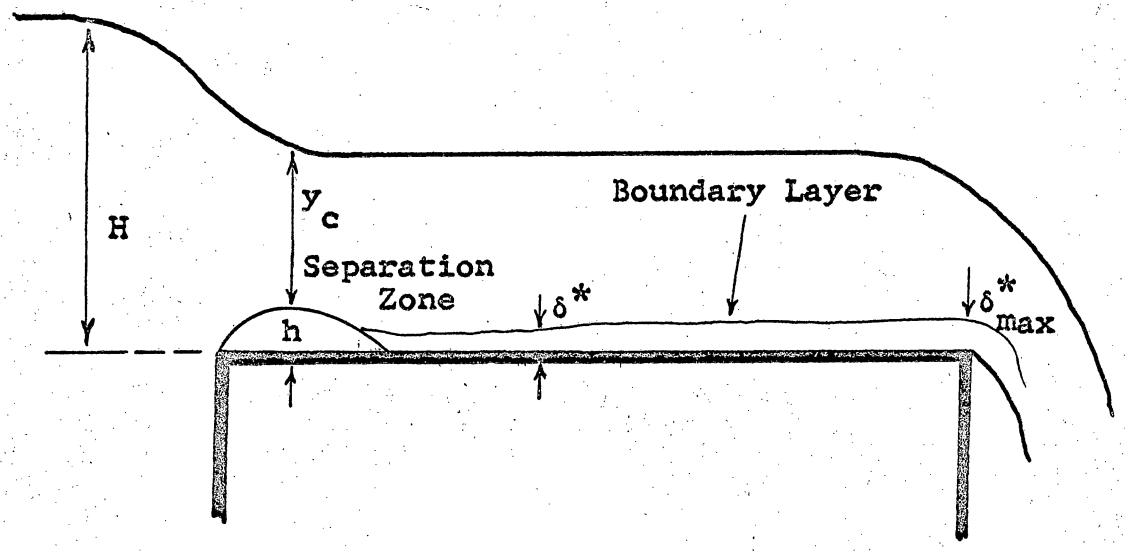

Figure 30. Probable Behavior of Crest Boundary Layer.

The assumption that the maximum separation height is the factor which causes critical flow to occur is supported by Woodburn (22) who observed the critical depth to be located at the upstream end of the weir.

For two-dimensional broad-crested weirs in which the height of the separation region controls the discharge, the effective head on the weir would be expressed by (H-h) instead of by ($H-\delta^*_{max}$) as in Eq. 7. To evaluate the discharge coefficient theoretically for the two-dimensional case would

thus require a method of predicting the maximum height of the crest separation zone. The analysis of the three-dimensional case would require the evaluation of the effective crest width which would involve the prediction of the maximum separation thickness on the side walls.

VII CONCLUSIONS

Hall's analysis fails to predict the correct value of the discharge coefficient C for a broad-crested weir with aspect ratios $\frac{B}{H}$ between 1 and 10 and for Reynolds numbers between 10,000 and 300,000.

The simplified flow model proposed by Hall is invalid because it assumes critical flow always to be located at the downstream end of the weir.

It is probable that for the values of the ratio $\frac{L}{H}$ encountered in the experiments, the factor determining the location of critical flow and thus controlling the discharge of the weir is the maximum height of the separation zone.

A complete theoretical analysis would require evaluation of the thickness of the separation zones on the crest and side walls of the weir and would relate these factors to the geometry of the weir, roughness of the upstream face and crest, and to the total head on the weir.

VIII BIBLIOGRAPHY

1. Addison, H. Hydraulic Measurements. New York: John Wiley and Sons, Inc., 1949. p. 242.

2. Blackwell, T.E. "Results of a Series of Experiments on the Discharge of Water by Overfalls or Weirs", Proceedings Institution of Civil Engineers (London), vol. X, 1851. p. 331.

3. Bradley, J.N. "Studies of Crests for Overfall Dams", Bulletin No. 3, Part VI, U.S. Bureau of Reclamation, Department of the Interior, Washington, D.C., 1948.

4. Chow, Ven Te. Open-Channel Hydraulics. New York: McGraw-Hill Book Co., Inc., 1959. pp. 52-53.

5. Delleur, J.W. "The Boundary Layer Development on a Broad-Crested Weir", Proceedings of the Fourth Mid-western Conference on Fluid Mechanics, Purdue University, 1955. pp. 183-193.

6. Fteley, A., and F.P. Stearns. "Experiments on the Flow of Water, Made During the Construction of Water of Sudbury River to Boston", Transactions, A.S.C.E., vol. 12, 1883. pp. 1-118.

7. Hall, G.W. "Analytical Determination of the Discharge Characteristics of Broad-Crested Weirs Using Boundary Layer Theory", Proceedings Institution of Civil Engineers (London), vol. 10, June 1962. pp. 177-188; and discussion, vol. 28, August 1964. pp. 514-548.

8. Harris, C.W. Hydraulics. New York: John Wiley and Sons, Inc., 1936. p. 53.

9. Hay, N., and E. Markland. "The Determination of the Discharge Over Weirs by the Electrolytic Tank", Proceedings Institution of Civil Engineers (London), vol. 10, May 1958. pp. 59-86.

10. Henderson, F.M. Open Channel Flow. New York: The Macmillan Company, 1966. pp. 36-37, p. 192, and p. 212.

11. Horton, R.E. "Weir Experiments, Coefficients, and Formulas", U.S. Geological Survey Water Supply and Irrigation Paper 200, 1907.

12. Ippen, A.T. "Channel Transitions and Controls", Engineering Hydraulics, ed. H. Rouse. New York: John Wiley and Sons, Inc., 1950. Chapter 8.

13. King, H.W. Handbook of Hydraulics, rev. E.F. Brater. New York: McGraw-Hill Book Company, Inc., 1954. p. 5-4.

14. King, H.W., C.O. Wisler, and J.B. Woodburn. Hydraulics. New York: John Wiley and Sons, Inc., 1948. p. 165.

15. Lea, F.C. Hydraulics. London: Edward Arnold and Company, 1938. p. 138.

16. Linford, A. Flow Measurement and Meters. London: E. & F.N. Spon Ltd., 1961. pp. 274-275 and p. 288.

17. Rafter, G.W. "On the Flow of Water Over Dams", Transactions A.S.C.E., vol. 44, Dec. 1900. pp. 220-398.

18. Rouse, H., and A.-H. Abul-Fetouh. "Characteristics of Irrotational Flow Through Axially Symmetric Orifices", Journal of Applied Mechanics, De., 1950. pp. 421-426.

19. Rouse, H., and S. Ince. History of Hydraulics. New York: Dover Publications, Inc., 1963. pp. 172-178.

20. Schlicting, H. Boundary Layer Theory, trans. J. Kestin. New York: McGraw-Hill Book Comapny, 1960. pp. 502-508 and pp. 534-537.

21. Schroder, E.W., and F.M. Dawson. Hydraulics. New York: McGraw-Hill Book Company, Inc., 1934. pp. 175-177.

22. Woodburn, J.G. "Tests of Broad-Crested Weirs", Transactions A.S.C.E., Paper No. 1797, 1932. pp. 387-408.

The vita has been removed from the scanned document

APPENDICES

APPENDIX A

Critical Flow Relations

The specific energy E is defined in open channel parallel flow as the energy of the flow referred to the channel bottom, or

$$E = y + \frac{v^2}{2g} \tag{1}$$

where y is the depth of flow, v is the average velocity, and g is the acceleration due to gravity.

For a rectangular channel,

$$q = vy \tag{2}$$

in which q is the discharge per unit width. Thus,

$$E = y + \frac{q^2}{2gy^2} \tag{3}$$

The definition of critical flow for a given unit discharge q is that flow for which the specific energy is minimum. At critical flow, therefore,

$$\frac{\partial E}{\partial y} = 0 \tag{4}$$

For a rectangular channel,

$$\frac{\partial E}{\partial y} = \frac{\partial \left(y + \frac{q^2}{2gy^2}\right)}{\partial y} = 1 - \frac{q^2}{gy^3} = 0$$

and

$$q^2 = gy_c^3 = (gy_c)y_c^2 \tag{5}$$

It follows from Eq. (2) that

$$q^2 = v_c^2 \, y_c^2$$

$$v_c^2 = g \, y_c \tag{6}$$

and

$$\frac{v_c^2}{2g} = \tfrac{1}{2}y_c \tag{7}$$

Also, since $E_c = y_c + \frac{v_c^2}{2g}$,

$$E_c = y_c + \tfrac{1}{2}y_c = \frac{3}{2} y_c \tag{8}$$

APPENDIX B

Discharge Measurement

Prior to the weir experiments, the venturi meter used to measure the discharge into the tilting flume was calibrated gravimetrically.

For this purpose, the entire flow from the constant-head tank was diverted by means of valves into a weighing tank whose total weight was indicated on a large circular dial. With water flowing continuously into the tank, a stop watch was started as the dial indicator passed a chosen initial weight and stopped when the indicator passed a selected final weight.

The initial and final weights were recorded along with the readings of the two venturi meter manometers and the elapsed time indicated by the stop watch. The manometers were read to the nearest 0.01 inch except when fluctuations were apparent; readings were then made to the nearest 0.1 inch. The elapsed time was recorded to the nearest 0.1 second.

Discharges were computed from the weight and elapsed time data using a specific weight of water of 62.4 lb/ft^3. Log-log plots of the discharges as functions of the manometer readings were used to obtain the following rating equations for the meter:

$$Q = 0.1930 \ (H_{Hg})^{0.5}$$

and

$$Q = 0.0775 \ (H_{2.95})^{0.5}$$

in which H_{Hg} is the reading of the mercury manometer and $H_{2.95}$ is the reading of the manometer containing manometer fluid.

APPENDIX C

Computer Programs

Data from the weir experiments and from the literature were analyzed by an IBM Model 7040 digital computer, using three separate programs:

Program 1	Analysis of test data (broad-crested weir)
Program 2	Analysis of test data (sharp-crested rectangular weir)
Program 3	Analysis of data from the literature.

The input data for Programs 1 and 2 consisted of observed heads H in inches and venturi meter manometer readings, also in iches. The geometrical parameters for the weir including length L, width B, and height P were not actual input data but were defined in the programs. The kinematic viscosity ν was also defined in each program and was changed manually when different water temperatures were encountered.

The input data to Program 3 included observed heads H in feet, unit discharges Q in cfs, and the crest length L, crest width B, and crest height P, all in feet. The kinematic viscosity was defined within the program.

Each program computed and printed some or all of eleven different variables as indicated by the following table:

	H	Q	U	RH	$\frac{L}{H}$	$\frac{B}{H}$	K	CC	CB	C	CEX
Program 1	x	x	x	x	x	x	x	x	x	x	x
Program 2	x	x	x	x							x
Program 3	x	x	x	x	x	x	x	x			x

H = Head in feet

Q = Discharge in cfs

U = Critical velocity v_c from Eq. (3)

RH = Reynolds number $R_H = \frac{v_c H}{}$

$\frac{L}{H} = \frac{L}{H}$

$\frac{B}{H}$ = Aspect ratio

K = Coefficient K in Eq. (20)

CC = Theoretical discharge coefficient C from Eq.(20)

CB = Theoretical discharge coefficient C_B from Eq.(26)

C = Theoretical discharge coefficient C_{TH} from Eq.(27)

CEX = Experimental discharge coefficient C_{EX}

The discharge Q was evaluated in Programs 1 and 2 from the venturi meter rating equations given in Appendix B. In Program 3, Q is a unit discharge and is read as input data.

The coefficient K was evaluated from Hall's relationship by the equation

$$K = 2.84 \cos (0.959 \frac{H}{H+P})$$

which proved to be accurate within the range of $\frac{H}{H+P}$ encountered.

The experimental discharge coefficient C_{EX} was evaluated for the broad-crested weir by the equation

$$C_{EX} = \frac{Q}{3.089\ B\ H^{3/2}}$$

which is based on Eq. (27).

For the sharp-crested weir, the following equation was used:

$$C_{EX} = \frac{Q}{5.350\ B\ H^{3/2}}\ .$$

```
C       PROGRAM 1

C       EVALUATION OF DISCHARGE COEFFICIENT FOR BROAD-CRESTED
C       WEIR. LENGTH OF WEIR = 3.0 FEET. WIDTH = 0.75 FEET.
C       KINEMATIC VISCOSITY BASED ON WATER TEMPERATURE OF
C       64.5 DEGREES FAHRENHEIT.
        DIMENSION  HG (100), RED (100 ), HIN (100)
        READ ( 5, 50 ) N
   50 FORMAT ( I 10 )
        READ ( 5, 10 ) ( HG(J), RED(J), HIN(J), J = 1, N )
   10 FORMAT ( 3 F 10.2 )
        WRITE ( 6, 20 )
   20 FORMAT ( 10X, 1HH, 8X, 1HQ, 8X, 1HU, 8X, 2HRH, 6X,
     1 3HL/H, 7X, 3HB/H, 8X, 1HK, 2HCC, 7X, 2HCB, 7X, 1HC,
     2 7X, 3HCEX )
        CREST = 3.0
        B = 0.75
        VISCOS = 0.00001048
        DO 30 J = 1, N, 1
        IF ( HG(J) .EQ. 0.0 ) Q = 0.0775 * RED(J) ** 0.5
        IF ( HG(J) .NE. 0.0 ) Q = 0.1930 *HG(J) ** 0.5
        H = HIN(J) / 12.0
        U = 4.6332 * SQRT (H)
        RH = U * H / VISCOS
```

```
      COEFF = 2.84 * COS ( 0.959 * H / ( H + 1.0 ) )
      RATIO = CREST / H
      CC = 1.0 - ((0.0690 * (RATIO - 1.0 + COEFF * RH **
     1 0.25 ) ** 0.8 ) / RH ** 0.2 )
     1 / RH ** 0.2 )
      ASPECT = B / H
      CB =  1.0 - ( 4.0 / ( 3.0 * ASPECT ) ) * ( 1.0 - CC )
      C = CC * CB
      CEX = Q / (3.0890 * B * H ** 1.5 )
   30 WRITE ( 6, 40 ) H, Q, U, RH, RATIO, ASPECT, COEFF,
     1 CC, CB, C, CEX
   40 FORMAT ( 7X, F 6.4, 3X, F 6.4, 2X, F 6.4, 2X, E 9.2,
     1 3X, F 4.1,  5X, F 6.3, 5X, F 5.3, 4X, F 6.4, 3X,
     2 F 6.4, 2X, F 6.4, 3X, F 6.4 )
      STOP
      END
```

```
C      PROGRAM 2

C      EVALUATION OF DISCHARGE COEFFICIENT FOR SHARP-CRESTED
C      RECTANGULAR WEIR. CREST WIDTH = 0.75 FEET. KINEMATIC
C      VISCOSITY BASED ON WATER TEMPERATURE OF 64.5 DEGREES
C      FAHRENHEIT.
       DIMENSION  HG (100), RED (100 ), HIN (100)
       READ ( 5, 50 ) N
   50  FORMAT ( I 10 )
       WRITE ( 6, 70 )
   70  FORMAT ( 10X, 1HH, 8X, 1HQ, 8X,1HU, 8X, 2HRU, 7X,
      1 3HCEX )
       B = 0.75
       VISCOS = 0.00001134
       DO 30 J = 1, N, 1
       IF ( HG(J) .NE. 0.0 ) Q = 0.1930 *HG(J) ** 0.5
       IF ( HG(J) .EQ. 0.0 ) Q = 0.0775 * RED(J) ** 0.5
       H = HIN(J) / 12.0
       U = 4.6332 * SQRT (H)
       RH = U * H / VISCOS
       CEX = Q / ( 5.350 * B * H ** 1.5 )
   30  WRITE ( 6, 80 ) H, Q, U, RH, CEX
   80  FORMAT ( 7X, F 6.4, 3X, F 6.4, 2X, F 6.4, 2X, E 9.2,
      1 3X, F 6.4 )
       STOP
       END
```

```
C      PROGRAM 3

C      EVALUATION OF DATA FROM LITERATURE FOR BROAD-CRESTED
C      WEIRS WITH 80RIZONTAL CRESTS AND SQUARE ENTRANCE
C      EDGES. KINEMATIC VISCOSITY BASED ON WATER TEMPERATURE
C      OF 64.5 DEGREES FAHRENHEIT.
       DIMENSION  Q ( 200 ), H ( 200 ), CREST ( 200 ),
      1 P ( 200 ), B ( 200 )
       READ ( 5, 50 ) N
   50 FORMAT ( I 10 )
       READ ( 5, 90 ) ( Q(J), H(J), CREST(J), P(J), B(J),
      1 J = 1, N )
   90 FORMAT ( 5 F 10.4)
       WRITE ( 6, 20 )
   20 FORMAT( 10X, 1HH, 8X, 1HQ, 8X, 1HU, 8X, 2HRH, 6X,
      1 3HL/H, 7X, 3HB/H 1HK, 8X, 2HCC, 8X, 3HCEX )
       BB = 1.00
       VISCOS = 0.00001134
       DO 30 J = 1, N, 1
       U = 4.6332 * SQRT ( H(J) )
       RH = U * H(J) / VISCOS
       COEFF = 2.84 * COS ( 0.959 * H(J) / ( H(J) + P(J) ))
       RATIO = CREST(J) / H(J)
```

```
      CC = 1.0 - ((0.0690 * (RATIO - 1.0 + COEFF * RH **
     1 0.25 ) ** 0.8 ) / RH ** 0.2 )
      ASPECT = B(J) / H(J)
      CEX = Q(J) / ( 3.089 * BB* H(J) ** 1.5 )
   30 WRITE ( 6, 40 ) H(J), Q(J), U, RH, RATIO, ASPECT,
     1 COEFF, CC, CEX
   40 FORMAT ( 7X, F 6.4, 2X, F 7.4, 2X, F 7.4, 1X, E 9.2,
     1 3X, F 5.1, 4X, F 7.3, 4X, F 5.3, 4X, F 6.4, 3X,
     1 F 6.4 )
      STOP
      END
```

APPENDIX D

Experimental Data

The data for the broad-crested and sharp-crested weir tests appear on the following pages.

EXPERIMENTAL DATA

HG = MERCURY MANOMETER READING IN INCHES
RED = MANOMETER-FLUID MANOMETER READING IN INCHES
HIN = HEAD ON WEIR IN INCHES

RUN 2 BROAD-CRESTED WEIR

HG	RED	HIN
55.55	0.0	9.73
43.85	0.0	9.05
37.82	0.0	8.65
32.25	0.0	8.19
28.95	0.0	7.90
25.60	0.0	7.60
22.45	0.0	7.27
18.65	0.0	6.85
15.35	0.0	6.41
12.05	0.0	5.95
0.0	61.75	5.51
0.0	48.13	5.06
0.0	36.85	4.64
0.0	26.90	4.18
0.0	20.43	3.79
0.0	14.04	3.35
0.0	8.28	2.85
0.0	6.70	2.67
0.0	4.55	2.28
0.0	3.15	2.00
0.0	1.70	1.65
0.0	1.00	1.38
0.0	0.72	1.25
0.0	0.50	1.10

EXPERIMENTAL DATA

HG = MERCURY MANOMETER READING IN INCHES
RED = MANOMETER-FLUID MANOMETER READING IN INCHES
HIN = HEAD ON WEIR IN INCHES

RUN 3 BROAD-CRESTED WEIR

HG	RED	HIN
56.65	0.0	10.0
51.00	0.0	9.55
44.55	0.0	9.13
38.15	0.0	8.67
30.35	0.0	8.05
22.80	0.0	7.30
16.75	0.0	6.60
12.48	0.0	5.98
0.0	55.20	5.30
0.0	40.50	4.79
0.0	31.61	4.40
0.0	18.90	3.70
0.0	14.20	3.35
0.0	9.41	2.92
0.0	5.05	2.36
0.0	3.15	2.01
0.0	1.68	1.65
0.0	0.70	1.23
0.0	0.25	0.90

RUN 4 SHARP-CRESTED WEIR

HG	RED	HIN
56.70	0.0	8.85
38.40	0.0	7.75
26.30	0.0	6.85
20.20	0.0	6.26
0.0	77.55	5.27
0.0	43.19	4.33
0.0	23.90	3.55
0.0	17.03	3.15
0.0	9.02	2.53
0.0	3.35	1.80
0.0	1.70	1.38
0.0	0.60	1.00

EXPERIMENTAL DATA

HG = MERCURY MANOMETER READING IN INCHES
RED = MANOM5TER-FLUID MANOMETER READING IN INCHES
HIN = HEAD ON WEIR IN INCHES

RUN 5 BROAD-CRESTED WEIR

HG	RED	HIN
56.65	0.0	9.90
47.60	0.0	9.33
36.30	0.0	8.55
24.90	0.0	7.53
16.60	0.0	6.58
0.0	59.75	5.45
0.0	46.41	5.00
0.0	32.31	4.44
0.0	20.91	3.84
0.0	9.15	2.90
0.0	5.85	2.50
0.0	2.18	1.79

RUN 6 BROAD-CRESTED WEIR

HG	RED	HIN
57.5	0.0	9.93
39.4	0.0	8.76
28.05	0.0	7.83
19.38	0.0	6.93
0.0	77.15	5.88
0.0	45.35	4.97
0.0	20.88	3.84
0.0	7.63	2.73
0.0	3.02	2.00

DISCHARGE COEFFICIENTS FOR BROAD-CRESTED WEIRS OF LOW ASPECT RATIOS

by

Carl Anderson

ABSTRACT

A previously developed theoretical analysis of the discharge coefficient for broad-crested weirs is investigated. Experimentally determined discharge coefficients are presented for a broad-crested weir of small crest width in an attempt to verify the theory, and an investigation of the geometry of the weir crest separation zone using a flow visualization technique is reported. Data from the literature for broad-crested weirs of large crest widths are also analyzed for comparison with the theory.

Correlation between the experimental coefficients and the theory is not evident and the geometry of the crest separation zone is not observed to conform to that assumed by the theory. Probable reasons for the failure of the theory are discussed and variables which should be included in further investigation are indicated.